ASSESSMENT OF WEATHER SENSITIVITIES AND AIR FORCE WEATHER (AFW) SUPPORT TO TACTICAL LASERS IN THE LOWER TROPOSPHERE

THESIS

Francesco J. Echeverria, Captain, USAF

AFIT/GAP/ENP/09-M05

DEPARTMENT OF THE AIR FORCE
AIR UNIVERSITY

AIR FORCE INSTITUTE OF TECHNOLOGY

Wright-Patterson Air Force Base, Ohio

APPROVED FOR PUBLIC RELEASE; DISTRIBUTION UNLIMITED

The views expressed in this thesis are those of the author and do not reflect the official policy or position of the United States Air Force, Department of Defense, or the United States Government.

AFIT/GAP/ENP/09-M05

ASSESSMENT OF WEATHER SENSITIVITIES AND AIR FORCE WEATHER (AFW) SUPPORT TO TACTICAL LASERS IN THE LOWER TROPOSPHERE

THESIS

Presented to the Faculty

Department of Engineering Physics

Graduate School of Engineering and Management

Air Force Institute of Technology

Air University

Air Education and Training Command

In Partial Fulfillment of the Requirements for the

Degree of Master of Science in Applied Physics

Francesco J. Echeverria, BS

Captain, USAF

March 2009

APPROVED FOR PUBLIC RELEASE; DISTRIBUTION UNLIMITED

AFIT/GAP/ENP/09-M05

ASSESMENT OF WEATHER SENSITIVITIES AND AIR FORCE WEATHER (AFW) SUPPORT TO TACTICAL LASERS IN THE LOWER TROPOSPHERE

Francesco J. Echeverria, BS

Captain, USAF

Approved:

Robb M. Randall (Chairman)	19 FEB 2009 Date
Steven T. Fiorino (Member)	19 MAR 09 Date
Richard J. Bartell (Member)	19 MAR 09 Date

Abstract

The Department of Defense (DoD) is spending millions of dollars on many Directed Energy (DE) programs. One of the programs, known as the Advanced Tactical Laser (ATL), requires the use of a high-energy laser in order to destroy ground targets from a standard C-130H aircraft. The ATL, which is still not fully operational and battle field ready, presents a great amount of potential for maintaining military superiority during wartime. One factor that affects the effectiveness of the ATL weapon system is that the operation of the ATL involves the propagation of a high-energy laser through an atmosphere that is made up of moving air molecules, cloud droplets, aerosols, and other weather phenomena.

ATL scientists need to develop a full understanding of the interaction effects between a high-energy laser beam and the atmosphere through which it propagates. Achieving this understanding is important for many reasons. In particular, the high cost of DE weapons systems makes each propagation event expensive. Having an understanding of the atmosphere in which a high-energy laser propagates will increase efficiency and effectiveness of the ATL weapon system, which in turn will decrease cost of operation. A tool that allows for the ATL war-fighter to determine the atmospheric effects on laser propagation currently does not exist. This study creates a stepping-stone toward creating a High Energy Laser Tactical Decision Aid (HELTDA) in which the war-fighter will be able to determine the effectiveness

of the ATL weapon system with accuracy in order to maximize efficiency in a specific environment.

Using the High Energy Laser End-to-End Simulation (HELEEOS) software, comparisons are made across various atmospheric factors. These factors consist of a variety of turbulence and wind profiles, aerosol effects, time of day, clouds and rain, and relative humidity, which are compared for summer and winter for a specific mid-latitude geographic location. In addition, the atmospheric factors run in HELEEOS are used to determine and characterize the relevant attenuating factors of extinction and thermal blooming, which are inferred by the different engagement scenarios tested.

The results illustrate the three attenuation factors of high energy laser propagation: optical turbulence, extinction, and thermal blooming. In this study, the most significant attenuation factor is thermal blooming. Extinction is a significant attenuator as well, however, not to the degree of thermal blooming. Optical turbulence proved to be a negligible attenuator for increasingly vertical engagements. This is especially true for ATL engagements, which are generally limited to approximately 10km in slant range. The seasonal and time of day weather effects are also at times significant.

Acknowledgments

I would like to thank God for giving me the strength and determination to complete the Applied Physics graduate program at the Air Force Institute of Technology. In addition, I am grateful for the opportunities that He has provided me and the courage He has given me to pursue these opportunities. I would also like to thank my mother, father, brothers, and sister for providing me with encouragement during the many stressful moments experienced during this research. Furthermore, I would like to thank Lt Colonel Steven Fiorino, Major Robb Randall, Mr. Matthew Krizo, and Mr. Richard Bartell for the guidance they provided me during this research. I would also like to thank Captain Seth Marek for his help and friendship while at AFIT in which my experience at AFIT would have been much different without having known him. Lastly, I would especially like to thank my wife and son for always reminding me of the important things in life.

Table of Contents

Page

List of Figures

List of Tables

Table Page

List of Acronyms

ABL	Airborne Laser
ADA	Atmospheric Decision Aid
AFW	Air Force Weather
AO	Adaptive Optics
ATL	Advanced Tactical Laser
BL	Boundary Layer
CLEAR 1	Critical Laser Enhancing Atmospheric Research
COIL	Chemical Oxygen Iodine Laser
DE	Directed Energy
DEEST	Directed Energy Environmental Simulation Tool
DoD	Department of Defense
ExPERT	Extreme and Percentile Environmental Reference Table
GADS	Global Aerosol Data Set
HEL	High Energy Laser
HELTDA	High Energy Laser Tactical Decision Aid
HELEEOS	High Energy Laser End-to-End Operational Simulation
HV 5/7	Hufnagel-Valley 5/7
ICBM	Intercontinental Ballistic Missiles
IR	Infrared
KAFB	Kirtland Air Force Base
OPAC	Optical Properties of Aerosols and Clouds
PDF	Probability Distribution Function
RH	Relative Humidity
SSL	Solid State Laser
SOR	Starfire Optical Range
STD	Standard
WPAFB	Wright Patterson Air Force Base

ASSESSMENT OF WEATHER SENSITIVITIES AND AIR FORCE WEATHER (AFW) SUPPORT TO TACTICAL LASERS IN THE LOWER TROPOSPHERE

I. Introduction

Background

The Department of Defense (DoD) is spending millions of dollars with the development of laser and high power microwave weapons. There are currently many DoD programs to develop lethal and non-lethal tactical laser weapon systems, which are expected to be operational in the next decade and beyond. The difference between tactical laser weapons and laser weapons meant for more strategic, long range missions is that the tactical mission infers more surface and low altitude targets where weather and other atmospheric effects are more prevalent. Researchers in the development of tactical laser weapons are looking for ways to mitigate these effects in order to optimize the effectiveness of war-fighter applications. As a contrasting example, the Airborne Laser (ABL) has a strategic mission to defeat ballistic missiles in boost phase. As such it will fly at high altitudes, above most adverse weather, and will shoot targets above most weather effects as well. For this program, an Atmospheric Decision Aid (ADA) is already under development to optimize the effectiveness of the weapon system at the designated ABL altitudes of operation. Understanding the weather, atmosphere, and terrain effects on laser propagation requires researchers to assess and extrapolate the most

important factors in order to create a High Energy Laser Tactical Decision Aid (HELTDA). Similar to an ADA, the purpose of developing an HELTDA is to enhance the war-fighter's ability to use tactical lasers such as the Advanced Tactical Laser (ATL) as well as other lethal and non-lethal tactical laser weapons in the lower troposphere.

Problem Statement

The underlying problem statement is to assess seasonal and time of day weather effects on boundary layer (BL) high-energy laser (HEL) engagements at a mid-latitude location to demonstrate the need for a tactical decision aid for low altitude HEL operations.

Purpose

The purpose of the thesis topic is to characterize the lower troposphere at an example site in order to maximize the effectiveness of the ATL and other lethal and non-lethal DE weapon systems. By characterizing the weather and atmosphere via physically-based simulated engagements, the war-fighter is able to input specific weather characteristics, such as rain rate and visibility, and establish the ability and effectiveness of using tactical laser weapons in any given environment. The development of a HELTDA is essential, especially since there is already a development of an ADA for the ABL used to understand the effectiveness in high altitude conditions.

Motivation

The ability to provide the war-fighter an accurate analysis of laser propagation in the lower troposphere does not currently exist. Such procedures are being developed for the ABL, which flies at altitudes that are above the lower troposphere and "above the weather" (Narcisse, 2008). At this point, understanding the performance of tactical lasers

in the lower troposphere is limited due to the lack of research of the effects that certain weather characteristics have on high energy lasers in the lower troposphere. The high cost of DE weapon systems makes accurate analysis of weather and atmospheric effects on laser propagation critical. In a time where conventional warfare is changing from high collateral damage weapons (bombs and missiles) to low collateral damage weapons (high energy lasers and high powered microwave weapons), the ability to accurately predict the dynamics of the atmosphere and achieve optimum effects of DE weapon systems in the medium in which these new weapons operate is essential (Narcisse, 2008).

Approach

The analysis consists of many simulated engagements using the High Energy Laser End-to-End Operational Simulation (HELEEOS) software. The environmental factors considered are:

1. Visibility/Pollution/Aerosols: The maximum horizontal distance, over which the eye can clearly discern features such as runways, obstacles, navigation lights, etc. affected by small particles of dust, salt, water, and other materials suspended in the air.

2. Rain rate (i.e. No Rain, Light Rain, Heavy Rain, etc.): categorized in terms of depth per unit of time.

3. Clouds/Fog: characterized by cloud type and altitude. Fog is a distinct cloud type.

4. Slant Ranges: straight-line distances from the platform (i.e. aircraft) to the targets.

5. Optical Turbulence: defined as the refractive index fluctuations that cause a laser beam to spread, wander, and distort as it propagates through the atmosphere.

6. Geographic Location: single geographic mid-latitude location is Wright Patterson Air Force Base WPAFB/Dayton, OH.

7. Time of Day: 3 hour increments such as 0300-0600, 1200-1500, etc.

8. Wavelength: the wavelength of interest is 1.31525μm.

9. Other factors to consider include thermal blooming and atmospheric extinction (i.e. absorption and scattering), which are related to the visibility, pollution, and aerosols listed above.

II. Literature Review

The primary discussions in this chapter consist of defining the factors that determine the impact on tactical HEL propagation. These factors are known as the attenuation factors that include extinction, thermal blooming, and optical turbulence. In addition, this chapter also identifies the differences between the Airborne Laser (ABL) and the Advanced Tactical Laser (ATL), the energy and irradiance required to destroy an object, the High Energy Laser End-to-End Operational Simulation (HELEEOS) model, and the differences between molecular and aerosol extinction. Furthermore, this chapter also includes a comparison of absolute humidity and relative humidity (RH), and their relationship within the atmospheric boundary layer (BL). Turbulence will be discussed separately from the extinction factors because turbulence affects a propagated beam of light in a slightly different way than extinction, which will be discussed in depth below. The purpose of identifying the differences between the ABL and ATL is to understand how this research differs from other research documents that have been created for the ABL and thereby explains why ABL research cannot always be used for ATL engagements.

Airborne Laser v. Advanced Tactical Laser

Throughout American history, the United States military has always sought after achieving the finest in military weapons. From the invention of the semi-automatic machine gun to the atomic bomb, the U.S. military has always been in constant pursuit of the latest technological advancement in order to incorporate technology on the battlefield and maintain superiority over its adversaries. The desire for laser development and

technology has increased after the War in the Persian Gulf. The latest in military technological advancement deals heavily in the development and operation of laser weapons in the battlefield. Among many of the possibilities that have been brainstormed by scientists and engineers regarding laser technology, the idea of an airborne HEL has been identified as having tremendous potential for combat and defense missions in the battlefield. Two of the top HEL programs that the military is currently interested in are the Airborne Laser (ABL) and the Advanced Tactical Laser (ATL) programs. While both laser programs involve the use of a HEL system on an aircraft, they differ greatly in their capabilities.

The ABL system consists of a high-energy, chemical oxygen iodine laser (COIL) that has been mounted on a modified Boeing 747 aircraft. The purpose of the ABL weapon system is to detect, track, and shoot ballistic missiles of all types during their boost phase, causing them to fall back toward their respective launch areas. The ABL weapon system does not only consist of a single 1.315μm COIL, but actually uses several COIL modules in order to achieve the required megawatt-class power level necessary to destroy targets hundreds of kilometers away at an altitude of about 40,000 feet. In addition to the COILs used, the ABL weapon system also involves the use of two solid-state (SSL), kilowatt-class, 1.064μm lasers as well as several infrared (IR) sensors (Hecht, 2008).

The operational procedure of the ABL is to initially detect the exhaust plumes of a boosting missile with the IR sensors. After the missile is detected, one of the SSLs, known as the Tracking Illuminator, locks on the missile and determines a target point of vulnerability on the missile. Next, the second SSL, known as the Beacon Illuminator, is

fired in order to measure the optical turbulence between the ABL aircraft and the target. Since targets range as far as hundreds of kilometers, the atmospheric disturbances within that range are significant enough to affect the quality of the high-energy as it propagates through the atmosphere. Therefore, after the Beacon Illuminator makes its measurement, the Adaptive Optics (AO) system, which is also a necessary component on the aircraft, makes the necessary corrections in order to accurately point and focus on the target. Lastly, the high-energy COIL beam is sent out through a large 1.5m telescope that is located on the nose turret of the aircraft, which is allowed to rotate, and focuses the mega-watt energy on a pressurized area of the missile, causing the missile to eventually break apart (MDA, 2008).

Since the ABL system flies at altitudes of about 40,000 feet, it is only intended for air-to-air targets. The advantage of this restriction is that the atmosphere at such altitudes is significantly less turbulent and relatively cloud-free, which allows the beam to propagate further with better beam quality. In addition, flying at such altitudes also means that the aircraft is above the portion of the atmosphere that contains aerosols and water vapor, two critical components that are responsible for attenuating the COIL. Another advantage of the ABL is that the aircraft can fly over friendly territory while scanning the horizon for possible targets. This is a major advantage because this reduces the threat of being shot down by enemy anti-aircraft. A disadvantage of the ABL weapon system is that the effectiveness decreases as the altitude decreases, which means that the ABL must stay at high altitudes of about 40,000 feet in order to maintain a high level of effectiveness (Wirsig and Fischer, 2008).

The other laser program of interest to the U.S. Air Force is the ATL, which is often dubbed as the Laser Gunship. Similar to the ABL weapon system, the ATL uses the 1.315μm COIL. However, rather than have six laser modules, each with an output power of a few hundred kilowatts, the ATL only requires one module to destroy its targets. The COIL is fitted into a standard C-130H gunship aircraft, the same type of four-propeller aircraft designed during the Korean War. The purpose of the ATL is to take out targets such as individual vehicles (i.e. trucks) as well as other ground targets such as cell phone towers and other communication targets. ATL can provide powerful capabilities for lethal and non-lethal engagements with precision and little or no collateral damage. One of the benefits of having a weapon system such as ATL, which operates below the clouds, is that the ATL provides the precision necessary to attack targets found in urban environments and congested chokepoints that are vulnerable to terrorist and insurgent operations. This precision is beneficial especially when there is the potential of collateral damage using standard conventional weapons (Rutherford, 2008).

The method of striking a target is similar to that of the ABL in the way that a high amount of energy is focused onto a specific area of the target. However, the ATL differs from ABL in range and altitude in which the aircraft operates. The range of the ATL is about 18-20km, depending on the time of year and location of operation. Interestingly enough, the range of the ATL is much more dependent on the atmospheric profile, which depends on factors such as geographic location, time of year, and time of day, in which the ATL operates. This contrasts sharply with the ABL primarily because the ABL is an air-to-air weapon system that operates above the troposphere and the ATL is an air-to-ground weapon system that operates in the extremely varying, lower troposphere. The

air-to-air versus air-to-ground capability is also evident in the location of the turret on each of the respective aircraft, shown in Figure 1 (Rutherford, 2008).

1a.

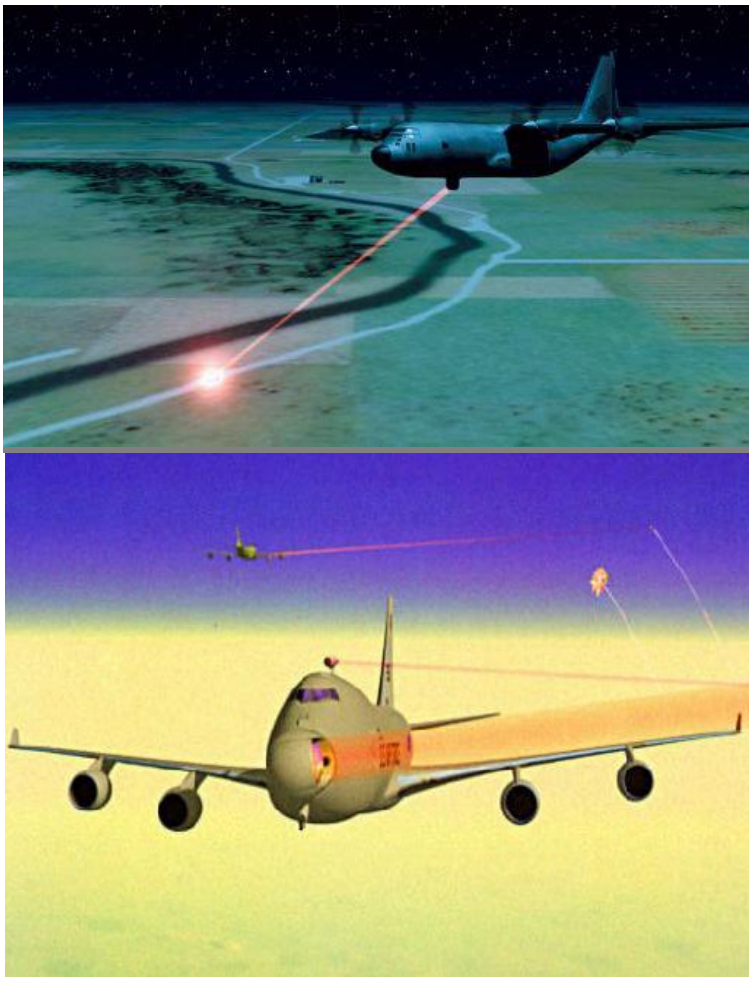

1b.

Figure 1. ABL v. ATL. The ATL (1a.) engages a target on the ground. The turret on the ATL is located underneath the aircraft. The ABL (1b.) flies above the lower troposphere and engages targets such as intercontinental ballistic missiles (ICBMs). The turret on the ABL is located on the nose of the aircraft. Courtesy of Popular Science Magazine and the United States Missile Defense Agency. http://www.popsci.com/scitech/article/2004-06/advanced-tactical-laser

One of the main factors that affect ATL engagements that the ABL does not face is the laser beam propagated from the ATL traverses through many kilometers of atmosphere containing attenuating elements such as aerosols, pollutants, and the varying types of weather and moisture that occur in the lower troposphere. This thesis will

primarily focus on those elements that affect the beam quality of the ATL as it propagates through various ranges in the lower troposphere region shown in Figure 2.

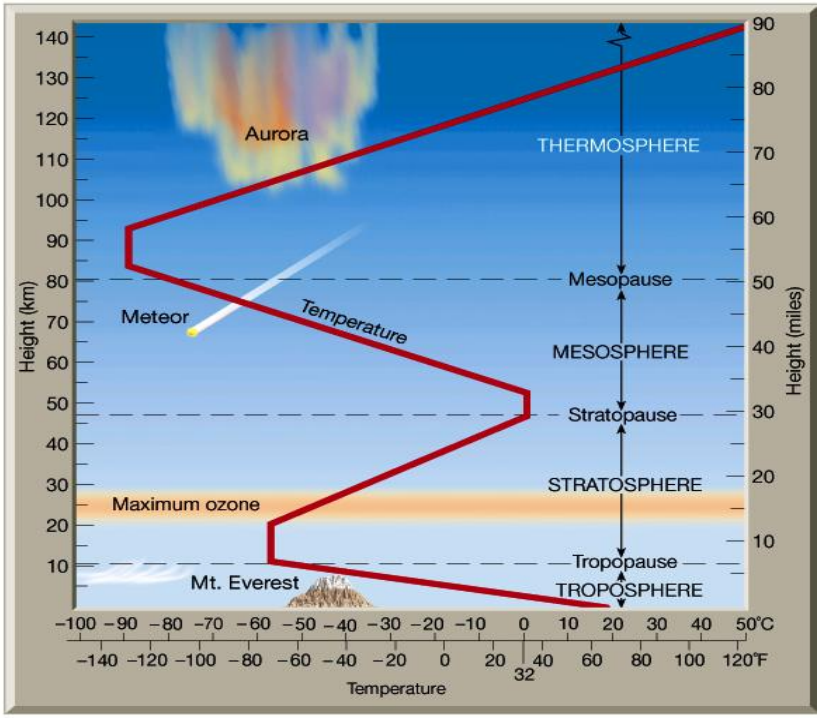

Figure 2. Layered Atmosphere. Solid line represents height versus temperature. The ATL operates in the lowest layer of the atmosphere, known as the troposphere, at maximum altitudes of approximately 5km. Observe that the temperature decreases with height in this region (Narcisse, 2008).

Energy Requirements

There is a certain amount of energy required to compromise the integrity (i.e. penetrate) of a certain material. In addition, different materials vary in energy requirements for puncturing the material and destroying the target. In order to understand the application of this concept, the method in which energy is transported and how energy interacts with surfaces must be defined. Ultimately, the parameter of concern in penetrating and destroying an object is known as fluence, which is the amount of power applied to a specific area for a given amount of time. Fluence is calculated by a simple

multiplication of irradiance, or flux density, measured in $W \cdot m^{-2}$, and dwell time, that is applied to a given surface. Irradiance (for the case of ATL) is defined as the amount of power per unit area on a given plane surface. Dwell time is defined as the amount of time, usually measured in seconds, for which the laser beam can be maintained on the same specific area. Understanding that the irradiance is dependent on output power and area on target is important because increasing the output power of the laser system or decreasing the focused spot size of the beam on the target can increase irradiance on the target. For the purpose of this research, the minimum fluence required to destroy a target is a parameter that can be input by the war-fighter for any target of choice. For typical ATL engagements, one can assume that the focused area on the target, known as the bucket area, is a fixed spot diameter less than or equal to 10cm (Bartell, 2008). It is convenient to assume a bucket area on the target for the purpose of calculating the power in bucket. This is done by using a form of Beer's Law (Petty, 2006) to relate the aperture exit power to the power in bucket. Conceptually, the equation for power in bucket that is most relevant for our discussion is as follows:

$$P = P_0 \cdot e^{-\beta_e \cdot s} \tag{1}$$

Where P_0 is the power exiting the aperture of the laser system and P is the power in bucket. In addition, s is the range from the laser aperture to the target and β_e is known as the total extinction coefficient, which is discussed in the Extinction Effect v. Slant Range section in more detail (Petty, 2006). The power in bucket divided by the area of the

bucket and multiplied with dwell time yields a fluence value in $J \cdot m^{-2}$, which is given by the expression:

$$\varphi = \frac{P}{(bucket\ area)} \cdot t \rightarrow P = \frac{\varphi \cdot (bucket\ area)}{t} \quad (2)$$

From this equation, knowing the minimum fluence value (φ) required to destroy a target and the maximum dwell time *t* that the laser system is capable of maintaining allows for the determination of the minimum amount of power necessary to achieve a successful kill, assuming a bucket with diameter less than or equal to 10cm.

Attenuation Factors

The main concern with propagating a laser through the lower troposphere is the meteorological elements that the laser beam interacts with in its propagation path; elements that the laser beam normally does not encounter or interact with if propagated above the lower troposphere where the ABL operates. A heavy concentration of this research consists of testing (via simulation) the various possible factors that produce significant attenuation; factors that should be accounted for when creating a High Energy Laser Tactical Decision Aid (HELTDA) for the ATL war-fighter.

Such possible factors include air molecules, cloud droplets, atmospheric aerosols, winds and weather (light rain, heavy rain, etc.). The existence of these factors in the atmosphere makes it virtually impossible for a laser beam to propagate through the lower troposphere without attenuation to some degree. It is imperative to understand and characterize each possible factor in order to determine the capabilities of the ATL weapon system in a given environment. The simulation model used to test these factors

also allows for testing in various geographic locations and time of day, since the concentration of certain air particles, aerosols, visibilities, weather, etc., vary at different locations and times of day around the planet. Importantly, simulated testing provides a low-cost, low-risk, and reasonable assessment of the significance of each parameter to create an effective HELTDA for the ATL war-fighter. The three attenuation factors investigated in this research are optical turbulence, extinction, and thermal blooming.

Extinction Effect v. Slant Range

As a beam of light is attenuated as it propagates through the atmosphere. Atmospheric extinction occurs in the lower troposphere due to the existence of aerosols and gas molecules in the atmosphere. Aerosols are defined as small solid and/or liquid suspended particles and do not include cloud droplets. Aerosols stay suspended due to their negligible terminal velocities. The extinction, which consists of absorption and scattering in the atmosphere, is linearly proportional to the intensity of the radiation (i.e. the propagated laser beam) along the path of propagation. In addition, extinction is linearly proportional to the local concentration and effectiveness of the gases and/or particles encountered along the propagation path causing the absorption and scattering. Therefore, extinction changes when either the intensity of the radiation (i.e. the power of the laser beam in the case of the ATL), the concentration of gas and/or aerosols along the beam path, or the effectiveness (i.e. such as size of particles) of the scatterers and absorbers change (Wallace and Hobbs, 2006). This concept is extremely important in understanding the quality of the beam reaching the target, which gives an understanding of the ATL system's lethal capabilities.

In order to characterize the total extinction along a certain propagation path and understand the contributions that scattering and absorption have on the total extinction, consider the extinction coefficient (β_e) in the following relationship (Petty, 2006):

$$\beta_e = \beta_a + \beta_s \tag{3}$$

Where β_a is the absorption coefficient and β_s is the scattering coefficient, all measured in units of inverse length (km^{-1}). Conceptually, absorption is the conversion of the propagated energy to heat or chemical energy as the propagated energy interacts with the particles in its path. Scattering is the redirection of the propagated energy out and away of the original direction of propagation, once again as a result of the interaction of the particles in the original path of propagation (Petty, 2006).

Understanding extinction is important, but the application of the concept of extinction is best understood when it is combined with transmittance (*t*). The simplest way to define transmittance is by explaining the values that it can possess. Transmittance is a dimensionless quantity that ranges from 0 to 1, where a value of 1 implies a complete transmission of energy (i.e. zero extinction) and a value of 0 implies a complete and total extinction of the propagated beam (i.e. zero power in bucket). The relationship that exists between atmospheric extinction (β_e) and transmittance (*t*) can be illustrated in the following equation (Petty, 2006):

$$t(s_1, s_2) \equiv e^{-\tau(s_1, s_2)} \tag{4}$$

Where s_1 and s_2 are the starting and ending points of the propagation path and τ is a dimensionless quantity known as the optical path (also known as the optical depth or optical thickness) defined as the integral of the total extinction as a function of the path length (s) between the starting point s_1 and ending point s_2 of propagation given by the equation (Petty, 2006):

$$\tau(s_1, s_2) \equiv \int_{s_1}^{s_2} \beta_e \, ds \tag{5}$$

Rewriting Equation (1) results in an equation that relates the power exiting the aperture (i.e. from the platform), the minimum power in bucket required to destroy target, and the total extinction coefficient for the maximum slant range that corresponds to the minimum power in bucket required to penetrate the target as the laser beam propagates through the atmosphere. However, since the atmosphere in the lower troposphere consists of many layers of various particles, it is insufficient to assume that the total extinction of the propagated beam is uniform throughout the propagated path. This is primarily the reason there must be an integration factor (i.e. Equation (5)) to account for all of the changes in extinction a beam of light undergoes as it travels from s_1 to s_2 (i.e. the slant range). The equation that yields slant range by rewriting Equation (1) is as follows:

$$s = \frac{-\ln(P/P_0)}{\beta_e} = \frac{-\ln(P/P_0)}{\beta_a + \beta_s} \tag{6}$$

From this equation, one can determine the maximum slant range from the platform exit aperture power of the laser beam, the minimum required power in bucket to penetrate the specific target, and the total extinction that the laser beam will experience throughout the path. One problem is the total extinction coefficient parameter (β_e) varies vertically as the slant range changes. In addition, while calculating the absorption coefficient (β_a) is quite straight forward, calculating the scattering coefficient (β_s) is difficult. In order to negotiate the two dimensional problem with the slant range, it is convenient to modify the slant range (*s*) parameter such that the war-fighter can input more convenient values such as altitude and slant angle. This adjustment allows the transmittance and optical depth to be strictly dependent on the vertical (*z*) parameter. Using a plane parallel approximation by assuming that all relevant radiative properties depend strictly on the vertical coordinate (*z*) and ignoring the curvature of the Earth due to the nature of ATL engagements, an equation is derived from Figure 3 and is written as follows (Petty, 2006):

$$s = z/\mu \;\; | \;\; \mu = |\cos\theta| \tag{7}$$

Note that the parameter μ depends on the zenith angle from the target to the aircraft, which is the same as the slant angle from the aircraft (vertically downward) to the target (See Figure 3). Substituting Equation (7) into Equations (4) and (5) yields:

$$t(z_1, z_2) = \exp\left[-\frac{1}{\mu}\tau(z_1, z_2)\right] \tag{8}$$

$$\tau(z_1, z_2) = \int_{z_1}^{z_2} \beta_e(z)dz \tag{9}$$

From Equations (8) and (9), the war-fighter can determine the transmittance from the aircraft to the ground as well as determine the optical depth, known as the optical thickness when strictly taken in the vertical direction (Petty, 2006).

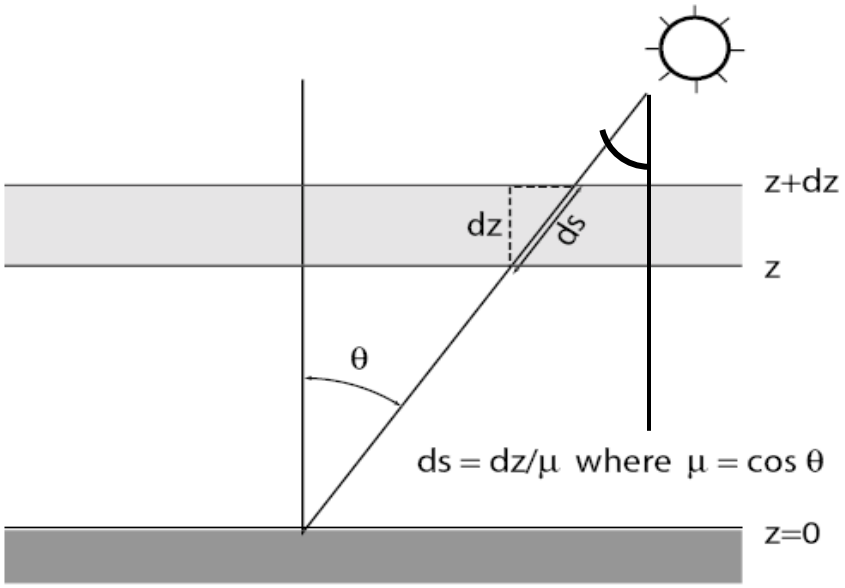

Figure 3. Relationship between slant and vertical paths in a plane parallel atmosphere. This approximation ignores horizontal variations in the structure of the atmosphere and assumes all relevant radiative properties depend strictly on the vertical (*z*) direction. In addition, the curvature of the Earth is ignored assuming a ray of light (or a laser beam) does not propagate at very oblique angles, similar to ATL engagements (Petty, 2006). Note that alternate interior angles are congruent.

By substituting Equation (7) into Equation (6), the following equation is derived:

$$z = -\frac{\mu \cdot \ln(P/P_0)}{\beta_e} \tag{10}$$

Rearranging Equation (10) yields the following equation:

$$\mu = -\frac{z \cdot \beta_e}{\ln(P/P_0)} \tag{11}$$

Equation (11) is useful because the war-fighter is ultimately solving for the maximum slant range. Since μ contains the slant angle (θ), then solving for μ by substituting into Equation (11) the corresponding input parameters of vertical distance (z), total vertical extinction (β_e), exit power (P_0), and minimum power in bucket (P), the war-fighter is able to use μ to calculate the maximum slant range using Equation (7). As far as the total vertical extinction is concerned, calculating a numerical value is difficult and beyond the scope of this thesis. For this value, the High Energy Laser End-to-End Operational Simulation (HELEEOS) software is used, which is discussed later in this review.

Thermal Blooming v. Slant Range

Thermal blooming is an effect of a self-induced phase distortion resulting in the distortion of the laser beam irradiance that occurs when a laser beam, generally of high power (i.e. >5kW) propagates through an absorbing medium. The absorbed laser beam energy, which is typically a very small fraction of the total laser beam energy, heats the medium causing localized gradients in the density. This changes the refractive index of the medium causing it to act as a distributed or thick nonlinear lens on the propagation of the laser beam. Since the heating of the absorbing medium results in the expansion of the medium and a decrease in refractive index in the region of the beam where the heating is the greatest, the beam is defocused and spread, as suggested by the term "blooming". The nature of thermal blooming effects on a laser beam depends on a number of factors such as laser beam characteristics (i.e. wavelength, continuous wave/pulsed, irradiance

distributions), the kinetics of the absorption process which determine the required time for the absorbed energy to heat the atmosphere, the mode of heat transfer that balance the absorbed energy (e.g. thermal conduction, free convection, forced convection), the time scale of interest, and the propagation medium and scenario characteristics (Gebhardt, 1990).

The underlying concept behind thermal blooming is that propagating a high-energy beam through an absorbing atmosphere, such as the lower troposphere, causes a change of the index of refraction in the atmosphere (i.e. the medium). The atmosphere then acts like a negative lens along the path of propagation, which causes the laser beam to diverge even more than usual. In addition, as the propagation path (slant range) increases, the amount of divergence of the beam resulting from thermal blooming increases. Furthermore, the temperature of the medium increases as more energy is absorbed along the propagation path. This increases the thermal blooming of the laser beam. As a result, a stationary beam yields a greater amount of thermal blooming due to the laser beam constantly heating the same section of medium along the propagation path. A laser beam in motion, however, via the motion of the ATL aircraft results in less heating of the atmosphere and less thermal blooming.

Optical Turbulence

Optical turbulence is defined as the refractive index fluctuations that cause a laser beam to spread, wander, and distort as it propagates through the atmosphere. Optical turbulence occurs due to the short duration small-scale temperature fluctuations, or eddies, in the atmosphere. Conceptually, optical turbulence causes objects viewed through a telescope to move, distant lights to twinkle, and objects viewed over hot

surfaces to shimmer (Pries, 1990). In Figure 4, the combination of warm and cold air mixes with eddies in the atmosphere causing a wave front that is initially flat (i.e. a plane wave) to quickly distort and become less effective on the target as the propagated distance increases (Wallace and Hobbs, 2006).

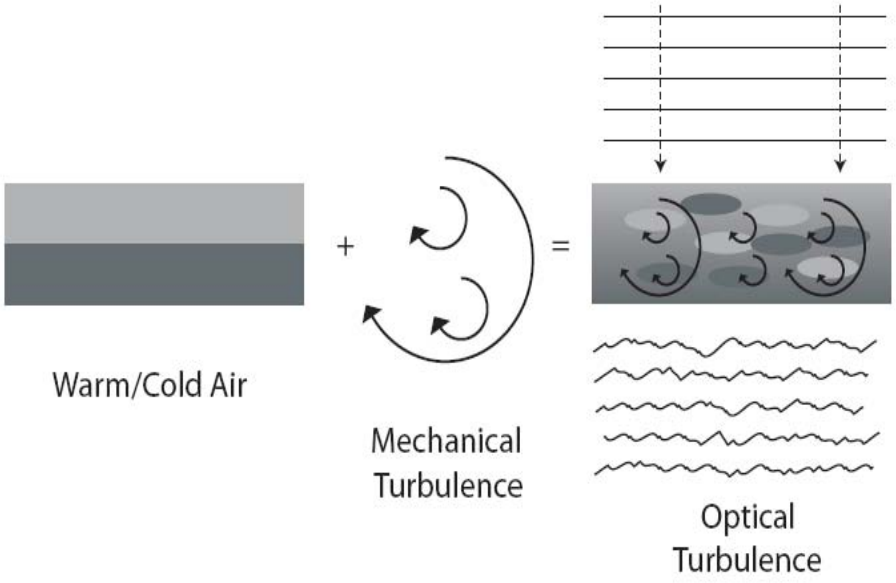

Figure 4. Composition of optical turbulence. Warm or cold air combines with mechanical turbulence and results in optical turbulence. An incident plane wave becomes distorted due to the interaction with optical turbulence. Courtesy of Air Force Institute of Technology METG 611 Optical Turbulence.ppt.

Much like a flowing river, the air in the lower troposphere can move quickly and violently or can be still or slow moving. In order to characterize the turbulent atmosphere in any given environment, scientists have developed a calculated value to determine the amount of turbulence between two points in the atmosphere known as the index-of-refraction structure constant (C_n^2) defined in the following equation (Pries, 1990):

$$\overline{n(\vec{r}_1) - n(\vec{r}_2)}^{\,2} = C_n^2 \cdot r^{2/3} \qquad (12)$$

Where n is the index of refraction and r is the separation distance between position vectors $\vec{r}_1$ and $\vec{r}_2$. It is important to recognize that a C_n^2 value characterizes the amount of turbulent spatial fluctuations due to temperature gradients in the atmosphere. In addition, an increase in C_n^2 value, which ranges from about 10^{-17} to 10^{-12} $m^{-2/3}$, is an increase in optical turbulence, which is used to understand the affect of refractive indices on laser wave fronts used in High Energy Laser propagation (Gravley et al, 2007). A C_n^2 value of 10^{-17} is a very weak or mild turbulent atmosphere while a C_n^2 value of 10^{-12} is a very strong and turbulent atmosphere.

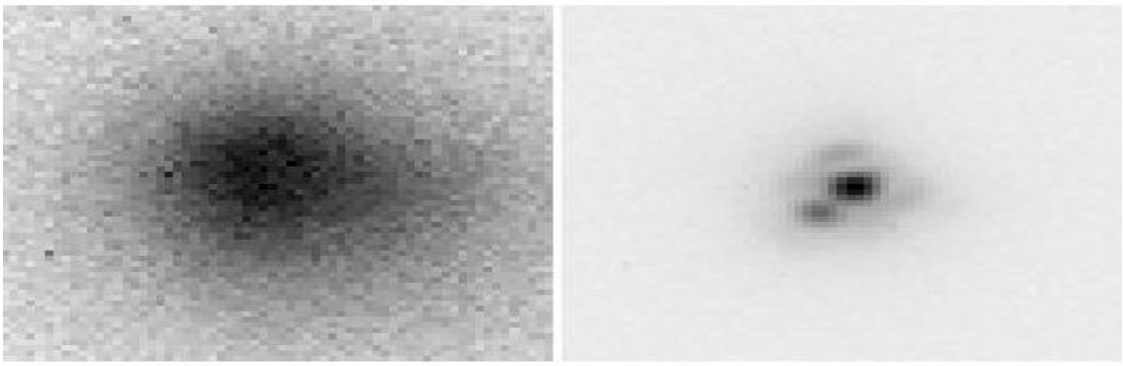

Figure 5. Optical Turbulence Effect. Left image is an object viewed through optical turbulence. Right image is the same object seen through an adaptive optics (AO) system. Note the difference in spreading as the image on the left appears larger in size than the image on the right. Courtesy of Air Force Institute of Technology METG 611 HELEEOS Overview.ppt.

In Figure 5, observe the affect of turbulence on the magnitude of irradiance reaching a target after traveling a certain distance through a turbulent atmosphere. The image on the right is a result of the wave front being corrected via the use of an Adaptive Optics (AO) system, which corrects for optical turbulence. A laser beam that propagates through a turbulent atmosphere results in less irradiance on target since the distribution is over a larger area on the target. It is important to note that turbulence is a separate

attenuation factor from extinction and thermal blooming. Turbulence alone can greatly reduce the irradiance on target, especially over very large distances (i.e. hundreds of kilometers), even if the extinction and thermal blooming through the atmosphere are non-existent. The combination of turbulence, extinction, and thermal blooming make tactical low altitude laser engagements more difficult to destroy a target.

High Energy Laser End-to-End Operational Simulation (HELEEOS)

The High Energy Laser End-To-End Operational Simulation, or HELEEOS, is a parametric one-on-one-engagement-level model that incorporates scaling laws tied to

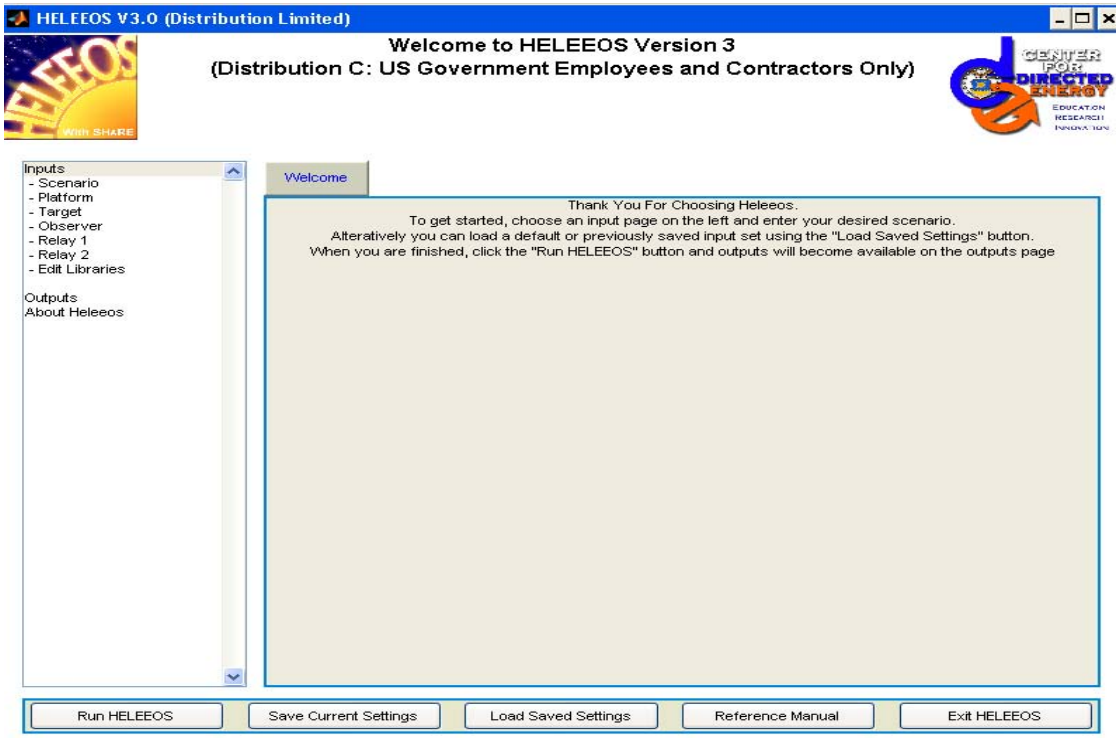

Figure 6. HELEEOS Model Main GUI. The HELEEOS model provides the user with a quick and accurate analysis of the operational environment. Courtesy of HELEEOS user guide.

respected wave optics codes and all significant degradation effects to include thermal blooming due to molecular and aerosol absorption, scattering extinction, and optical turbulence. The HELEEOS model enables the evaluation of uncertainty in low-altitude,

high-energy-laser (HEL) engagements due to all major atmospheric effects. Atmospheric parameters investigated include profiles of temperature, pressure, water vapor content, and optical turbulence as they relate to layer extinction coefficient magnitude. Worldwide seasonal, diurnal, and geographical spatial-temporal variability in these parameters are organized into probability density function (PDF) databases using a variety of available resources to include the Extreme and Percentile Environmental Reference Tables (ExPERT), the Master Database for Optical Turbulence Research in Support of the Airborne Laser, the Global Aerosol Data Set (GADS), and the Directed Energy Environmental Simulation Tool (DEEST) in conjunction with Air Force Weather Agency MM5 numerical weather forecasting data. Updated ExPERT mapping software allows the HELEEOS operator to choose from specific site or regional surface and upper air data to characterize correlated molecular absorption, aerosol absorption and scattering, and optical turbulence by percentile. The PDF nature of the HELEEOS atmospheric effects package enables realistic probabilistic outcome analyses that permit an estimation of the level of uncertainty in the calculated probability of kill. HELEEOS users can additionally access, display, and export the atmospheric data independent of a HEL engagement simulation (Gravley et al, 2007).

HELEEOS has the capability for providing the ATL war-fighter with a quick and accurate analysis of the specific operational environment. HELEEOS output provides the war-fighter information to evaluate the specific capabilities of the ATL weapon system such as effectiveness and range. Using the HELEEOS model, the ATL war-fighter is able to input parameters such as extinction, optical turbulence, and dwell time to

determine the irradiance on target, or power in bucket, and the corresponding maximum slant range that is expected in a real-world ATL engagement.

Molecular and Aerosol Extinction

Understanding molecular and aerosol extinction is important because of their involvement in affecting a propagated laser beam through the atmosphere. HELEEOS computes molecular scattering based on Rayleigh theory (Fiorino et al, 2007); in which the forward and backward scattering of the incident radiation are closely symmetric. Aerosol scattering and absorption are computed by HELEEOS using the Wiscombe (1980) Mie module (Fiorino et al, 2007), in which the majority of the scattering occurs in the forward direction with little scattering occurring in the backward direction. A geometric representation of the scattered incident radiation on a molecule and aerosol particle is in Figure 7.

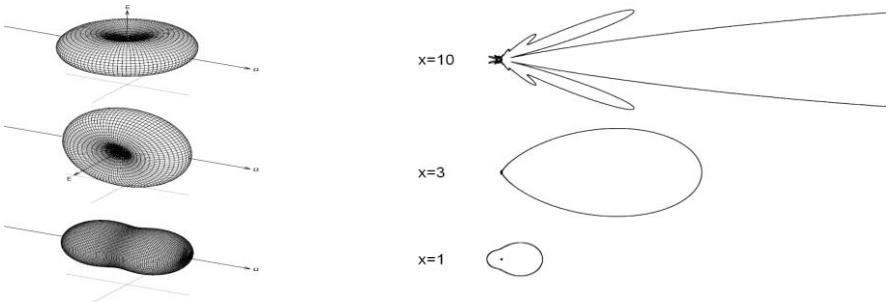

Figure 7. Rayleigh v. Mie Scattering. Rayleigh scattering (left) occurs in the atmosphere by the interaction of light (polarized or unpolarized) with air molecules. Notice that the maximum scattering occurs at 90° (radially outward) with the polarized E-field for vertically polarized light (left top) and horizontally polarized light (left middle). Unpolarized light (left bottom) results in maximum scattering in the forward and backward directions only. Mie scattering (right) occurs in the atmosphere by the interaction of light with aerosols. Notice the scattering occurs predominately in the forward direction. The x-values represent the size parameter of the particles as a function of radius of particle and wavelength of incident light given by $x = 2\pi r/\lambda$. In addition, the magnitude of the forward scattering increases as the size of the particle increases (as is shown by the x-values) for a given wavelength (Petty, 2006).

An important feature to notice from the molecular scattering (i.e. Rayleigh profile) is that unpolarized incident radiation will scatter in all directions with a greater

percentage of the scattered light in the forward and backward direction. Incident radiation that is vertically polarized will scatter in all directions except vertically, with the greatest percentage of scattered light being in the horizontal direction (i.e. with respect to a vertically polarized electric field). Similarly, incident radiation that is horizontally polarized will scatter in all directions except horizontally, with the greatest percentage of scattered light being in the vertical direction (i.e. with respect to a horizontally polarized electric field). In addition, aerosol scattering (i.e. Mie profile) occurs primarily in the forward direction. As the aerosol particle gets larger, the amount of forward scattering from the incident radiation at constant wavelength increases while the amount of backward scattering decreases (Petty, 2006). In HELEEOS, the molecular absorption effects are computed for the top 13 absorbing species such as carbon dioxide (CO_2), water vapor (H_2O), ozone (O_3), methane CH_4), and nitrous oxide (N_2O), using line strength information from the HITRAN 2004 database (Fiorino et al, 2007).

The HELEEOS model uses a diverse array of aerosol vertical profiles as well. The aerosol profiles compared in this study include 4 profiles defined using the Optical Properties of Aerosols and Clouds (OPAC) code (Hess et al, 1998) as well as the Global Aerosol Data Set (GADS) profile (Koepke et al, 1997). The continental clean aerosol profile represents remote continental areas with less than $0.1\mu g \cdot m^{-3}$ of soot. The continental average aerosol profile is used to represent continental areas containing soot and an increased amount of the insoluble and water-soluble components. The continental polluted aerosol profile represents areas that are highly polluted by man-made activities. The mass density of soot in these areas is $2\mu g \cdot m^{-3}$ with double the mass density of water-soluble substances in continental average aerosol profile areas. The urban aerosol profile

represents a strong pollution in urban areas. The mass density of soot is $7.8\mu g \cdot m^{-3}$ with mass densities of water-soluble and insoluble substances being about twice the amount found in continental polluted aerosol areas (Hess et al, 1998). The GADS aerosol profile provides aerosol constituent number densities on a 5° by 5° grid worldwide (Fiorino et al, 2007). The GADS profile is a suitable aerosol profile for analysis since the GADS profile provides worldwide aerosol constituent number density measurements.

Absolute Humidity v. Relative Humidity

In studying the effects of the lower troposphere on a propagated laser beam, it is essential to understand the constituents that influence the climate in that section of the atmosphere. The most variable characteristic of the atmosphere that influences the climate and weather in the lower troposphere is water vapor. The presence of water vapor in the air and the vapor pressure that it exerts is critical in understanding the relationship between temperature, relative humidity, and absolute humidity.

Relative humidity is defined as the ratio, in percentage, of the amount of water vapor in a given volume of air relative to the amount of water vapor in the same volume of air at saturation, which always has a relative humidity of 100%. Absolute humidity is defined as the moisture density in a given volume of air, which is usually measured in grams per cubic meter. Mathematically, RH is calculated using the following equation (Wallace and Hobbs, 2006):

$$RH = {}^{e}\!\!\diagup\!\!{}_{e_s} \cdot 100 \tag{13}$$

Where e is the vapor pressure and e_s is the saturation vapor pressure over a plane surface of pure water at temperature T. An increase in temperature corresponds to an increase in

saturation vapor pressure, thus more moisture may be present as water vapor before saturation (RH = 100%) occurs. This means that a volume of air with a fixed amount of moisture density (i.e. absolute humidity) will increase in relative humidity if the temperature of the air decreases, and conversely, the relative humidity will decrease if that same volume of air increases in temperature. This relationship allows two volumes of air with identical absolute humidity the ability to have different relative humidity. Similarly, two volumes of air can have identical relative humidity and have different absolute humidity, both cases depending primarily on the temperature of the volumes of air.

The relationship between temperature, absolute humidity, and relative humidity plays a significant role in understanding the amount of water vapor that is in the atmosphere. In the summer, when temperatures are high, a low relative humidity may still imply a large amount of water vapor or absolute humidity in the atmosphere, especially at low altitudes near the surface of the Earth. Similarly, in the winter, when temperatures are low, a high relative humidity may imply that the amount of water vapor in the atmosphere is very low because cooler air has a lower saturation vapor pressure. This relationship is very important in understanding the relative humidity effect on a propagated laser beam and is discussed in Chapter IV.

Atmospheric Boundary Layer

The atmospheric boundary layer (BL) is defined as the portion of the atmosphere that is most affected by the surface of the Earth. The thickness of the BL is approximately 1 to 2km thick under normal atmospheric conditions but can range from tens of meters to 4km thick. An understanding of the BL is absolutely essential for ATL

engagements because the BL will always be a section of the troposphere in which the laser must propagate through to destroy ground targets.

The three most relevant components of the lower troposphere for the purpose of ATL engagements are the BL, the capping inversion layer, and the free atmosphere. The layer of free atmosphere is a stable layer above the capping inversion layer and BL. The layer of free atmosphere is the portion of the Earth's atmosphere that is static, stable, and not affected or influenced by the surface of the Earth. The capping inversion layer, also a stable layer, separates the free atmosphere from the BL. The capping inversion layer is the part of the atmosphere that is created by the turbulent BL beneath and the static free atmosphere above. The capping inversion layer separates the turbulent, non-stable BL from the static, stable free atmosphere. In addition, the capping inversion is responsible for trapping turbulence, pollutants, and moisture within the BL. As a result, the BL is the layer in the lower troposphere that has the largest effect on a propagated laser beam. The processes that control the depth or thickness of the BL and cause it to evolve in response to changing environmental conditions are essential in understanding the effect of the BL on a propagated laser beam (Wallace and Hobbs, 2006).

In the summer time at sunrise, the warmed ground gradually heats the neighboring air and causes intense mixing, turning the stable BL into a convective unstable boundary layer. Just before sunset, the boundary layer is thickest and most turbulent due to the increased temperature and wind speed conditions throughout the day. Around sunset, the ground begins to cool to temperatures less than the neighboring air above. This cooling, which occurs throughout the evening and into the night, results in the formation of a stable boundary layer near the surface of the Earth. Above this stable

boundary layer exists a layer that contains slowly decaying turbulence, residual heat, moisture, and pollutants that were mixed during the previous day known as a residual layer. As the cold surface of the Earth cools the neighboring air throughout the night, the bottom of the residual layer is slowly transformed into a gradually thicker stable boundary layer. Just before sunrise, the boundary layer then consists of a stably stratified, non-turbulent, boundary layer near the ground as a result of the surface of the Earth being colder than the air above throughout the night. This cycle then repeats itself daily under normal weather conditions. In the wintertime, the nights are longer than the day, which causes a thicker stable boundary layer than during the summer. This results in a much thinner mixed layer in the daytime, causing the top of the stable boundary layer to persist day and night (Wallace and Hobbs, 2006).

III. Methodology

The purpose of using HELEEOS in this study is to examine the variance in low-altitude laser weapon system (i.e. ATL) performance through a wide range of atmospheric conditions including clear air aerosols, clouds, fog, and rain for a specific output power. Ultimately, there are several parameters in HELEEOS that can be used in a variety of combinations to set up specific cases, or environments, which the ATL might encounter on the battlefield. The following outlines the methods used in determining the relevant atmospheric and weather parameters for the understanding and development of a High Energy Laser Tactical Decision Aid (HELTDA).

The geometry of the aircraft-to-target engagement is a factor due to the range limitation of the ATL weapon system. The geometry chosen is a result of a real world hypothetical engagement based on the effective HEL range of the ATL defined in Chapter II. Specifically, the simulated geometry consisted of a C-130 aircraft flying due north with a velocity of $50 m \cdot s^{-1}$ at an altitude of 5000m over WPAFB. It should be noted that a velocity of $50 m \cdot s^{-1}$, which is considered slow for a C-130, was chosen for convenience in demonstrating the attenuation effects of the atmosphere on a propagated laser beam. The target is initially located 15km away with a relative azimuth angle of 30 degrees from the aircraft heading. In addition, the geometry of the aircraft is held constant for every engagement scenario to ensure consistency in the data gathered when testing each parameter. The geometry of the target is held constant except when testing the thermal blooming effects between the platform and the target. The three target geometries tested are target velocities of $0 m \cdot s^{-1}$, $10 m \cdot s^{-1}$ north, and $10 m \cdot s^{-1}$ south. This is

to see the effects, if any, that occur if the platform is engaging a target that is stationary, moving in the same, or opposite direction of the platform. Figures 8-10 illustrate the geometry of the aircraft-to-target engagement.

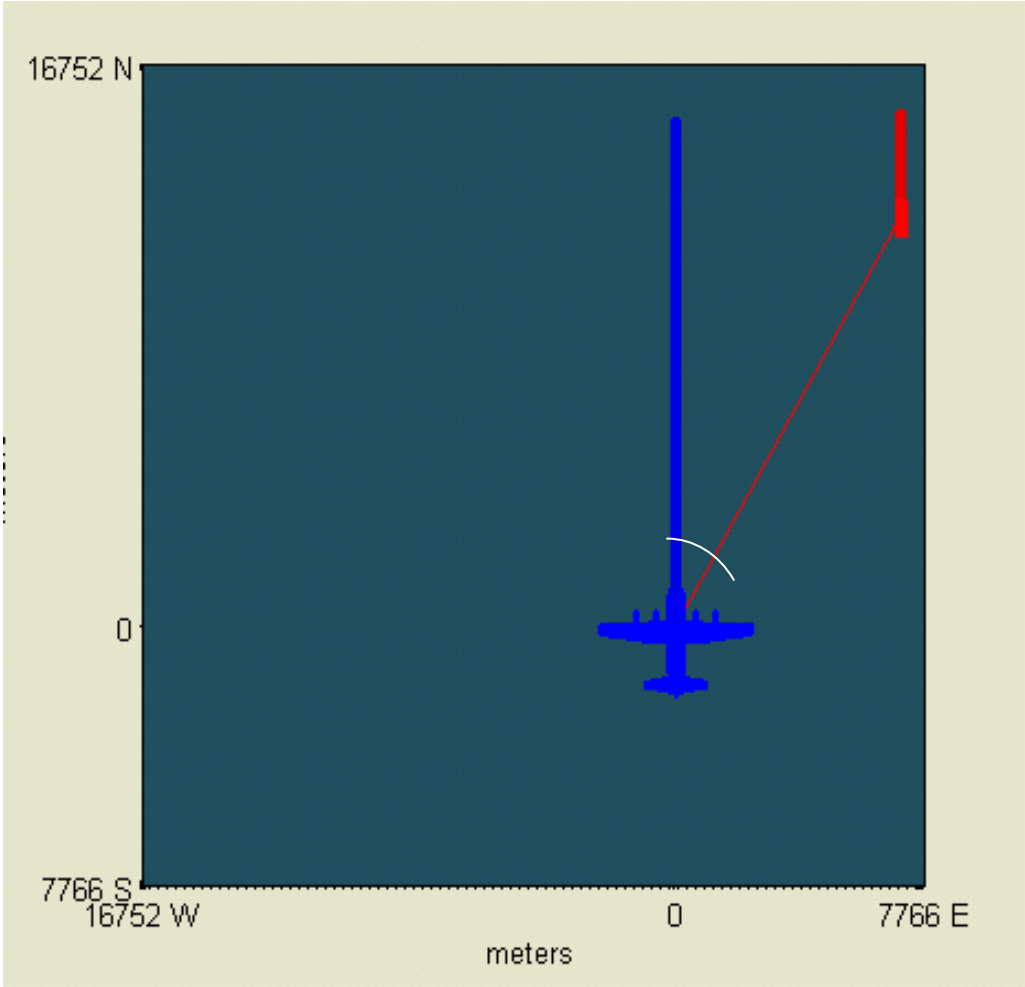

Figure 8. 2-D x-y static plane ATL geometry engagement. The "bird's eye view" of the ATL (C-130) engagement on the target shows the position at time t = 0s. The initial azimuth angle of the target relative to the aircraft is 30°. The platform and the target travel northbound as seen by the vertical and diagonal paths. For the stationary target, the red path is nonexistent. The red line connecting the aircraft to the target is the propagated laser beam at an initial slant range of 15km. Location is WPAFB, OH. Courtesy of HELEEOS 3.0.

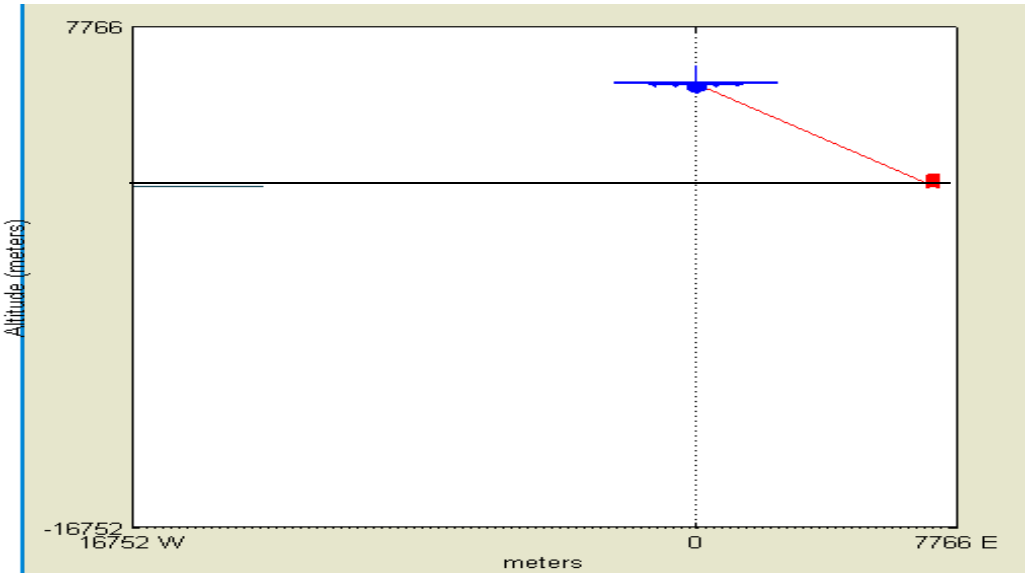

Figure 9. 2-D y-z static plane ATL geometry engagement. Aircraft is traveling north (into the page) and the target is stationary. The horizontal black line represents the ground and the aircraft has a constant altitude of 5km. Note that the southbound direction is out of the page. Location is WPAFB, OH. Courtesy of HELEEOS 3.0.

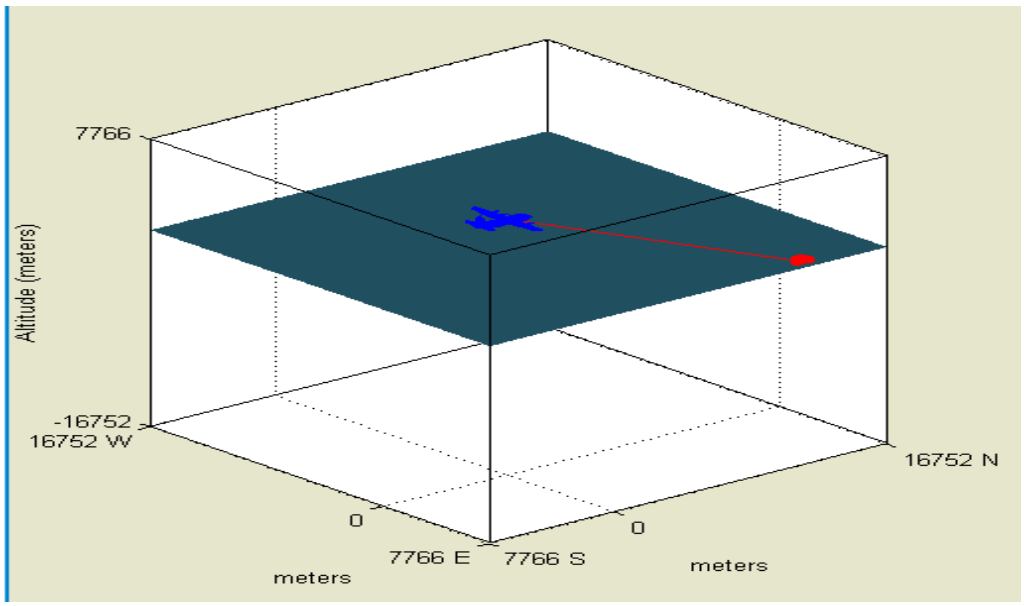

Figure 10. 3-D ATL geometry engagement. Aircraft travels north at a constant velocity of 50m·s^{-1} and the target is stationary. The red line connecting the aircraft with the target represents the propagated laser beam at an initial slant range of 15km. Location is WPAFB, OH. Courtesy of HELEEOS 3.0.

Each HELEEOS parameter is tested against each other in the analysis of a real world engagement scenario at WPAFB. The basic approach is to compare summer and winter engagements for each profile while keeping all other factors constant.

After establishing the appropriate profiles to use from the respective categories, the simulated laser engagements are carried out for various types of cloud and rain conditions. This is done by considering a cloud or rain depth below the aircraft. The purpose of this is to make a determination of condition(s) in which the ATL weapon system maintains an effective delivery of irradiance on target. In addition, varying the depths of the cloud and rain conditions in which the laser beam propagates is also essential, assuming that irradiance decreases as the atmospheric particles increase along the path of propagation. To show this effect, the four variations of cloud or rain depth considered are zero meters (i.e. 0 meters of clouds or rain below the aircraft or the clouds and rain above the aircraft), one-meter, 50 meters, and 500 meters below the aircraft.

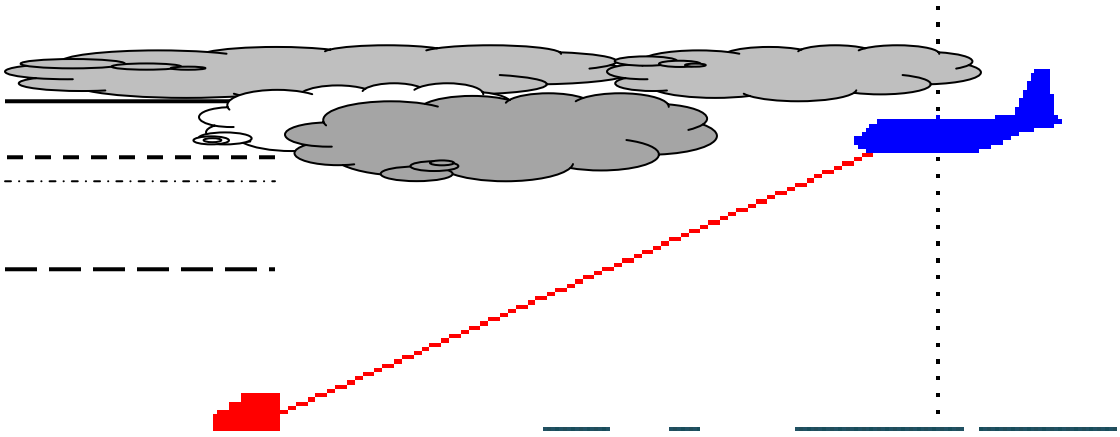

Figure 11. Cloud or rain depth variation. The cloud or rain condition varies in depth. Solid black line (on the left) represents cloud and rain depth of 0 meters below the aircraft. Short dashed line represents cloud or rain depth of 1 meter below the aircraft. Dashed-dot line represents cloud or rain depth of 50 meters below the aircraft. Long dashed line represents cloud or rain depth of 500 meters below the aircraft. Courtesy of HELEEOS 3.0.

The variations in cloud or rain depth are illustrated in Figure 11. The clouds shown in the figure represent clouds or rain. In addition, a cloud and rain depth assumes that the aircraft is traveling within the cloud or rain. This does not account for the case of the aircraft flying above the clouds or rain and propagating through the entire thickness of the clouds or rain. One should note the difference in a clear versus a cloud or rain atmosphere at the exit aperture of the laser. It is likely that the non-linear absorption effects (thermal blooming) may cause the extinction at the exit aperture to have more degrading effects on the beam at the target than if the same extinction existed at the target end of the beam. This case, however, is not examined in this research and is left for future study. While there are many factors that affect laser weapon system performance, HELEEOS allows for the reduction of relevant parameters through the analysis of simulated data. The atmospheric parameters tested are listed in Table 1.

Table 1. Run matrix of HELEEOS parameters.

Seasonal Depend.	Turbulence Profiles	Percentile RH	Time of day	Aerosol Effects Profile	Cloud and Rain Conditions	Cloud and Rain Depth	Target Dynamics
Summer	Hufnagel-Valley 5/7	1% Most Dry	0000-0300	Global Aerosol Data Set (GADS)	Cumulus Continental Clean	0 meters	Stationary
Winter	Clear 1	20%	0300-0600	Continental Average	Cumulus Continental Polluted	1 meter	10m·s^{-1} North
	Vacuum	50% Average	0600-0900	Continental Clean	Stratus Continental	50 meters	10m·s^{-1} South
	Climatological C_n^2 50th Percentile	80%	0900-1200	Continental Polluted	Fog	500 meters	
	Tunick	99% Most Damp	1200-1500	Urban Aerosols	Ice Fog		
	$C_n^2 = 0$		1500-1800	Clear (Unlimited Visibility)	Cirrus (-25 C)		
	SOR Special		1800-2100		Cirrus (-50 C)		
			2100-0000		Cirrus + Small Particles (-50 C)		
			Daily Average		Drizzle		
					Very Light Rain 2mm·hr^{-1}		
					Light Rain 5 mm·hr^{-1}		
					Moderate Rain 12.5 mm·hr^{-1}		
					Heavy Rain 25 mm·hr^{-1}		
					Extreme Rain 75 mm·hr^{-1}		

A determination of the relevant parameters that affect the performance of ATL engagements is done by analyzing the data developed by HELEEOS. Chapter IV provides a brief explanation of the parameters listed in Table 1. The purpose of these results is to create requirements for a HELTDA that is used to provide ATL planners/operators with a probabilistic approach for risk and effectiveness assessments of possible tactical engagements.

IV. Data Collection and Analysis

After running the HELEEOS software, the assumption that many atmospheric factors play a role in the performance of a laser weapon system is verified from the data. The main output parameters observed (i.e. independent v. dependent variables) are the peak irradiance on target ($W \cdot m^{-2}$) versus the slant range (meters) from the platform to the target in the simulated environment of WPAFB, OH. These parameters are of specific interest because of the relationship that exists between slant range and irradiance. By having a predetermined notion of the required irradiance on target, it is possible to determine a maximum slant range which the platform must maintain in order to achieve the desired effectiveness of the weapon system. It is important to recognize that all simulated engagements in this research consider atmospheric characteristics for WPAFB, OH. One must not misinterpret the results of this research as universal, since atmospheric profiles tend to vary with geographical location.

Optical Turbulence Profiles

Optical turbulence is defined as the refractive index fluctuations that cause a laser beam to spread, wander, and distort as it propagates through the atmosphere. The HELEEOS optical turbulence profiles that apply to ATL (i.e. continental) engagements are the Hufnagel-Valley 5/7 (HV 5/7), Critical Laser Enhancing Atmospheric Research (CLEAR 1), Vacuum, Climatological C_n^2, SOR Special, $C_n^2 = 0$ (constant C_n^2), and Tunick profiles. For ATL engagements, using a vacuum or $C_n^2 = 0$ optical turbulence profile is unrealistic since neither of these conditions occurs in the lower troposphere. Similarly, the SOR Special uses measurements taken at the Starfire Optical Range (SOR)

located at Kirtland Air Force Base (KAFB), New Mexico, which limits the accuracy of the SOR Special profile to similar environments. Furthermore, the Tunick optical turbulence profile applies to continental surface layers ranging from 0 to 100 meters, which is not an accurate representation for ATL engagements. The Climatological C_n^2 optical turbulence profile uses data collected in the Master Database for Optical Turbulence Research in Support of Airborne Laser. This database is obtained from thermosonde vertical profile measurements at various worldwide locations (Gravley et al, 2007). Since the mid-latitude Climatological C_n^2 optical turbulence profile uses observed data from mid-latitude sites, it represents the most realistic profile for optical turbulence. However, the measurements used in developing the Climatological C_n^2 optical turbulence profile are obtained strictly at night to avoid solar contamination of the data. Consequently, the most widely accepted optical turbulence profiles by the DoD are the standard (STD) models HV 5/7 and CLEAR 1 profiles (Gravley et al, 2007). Therefore, the optical turbulence profile used for the analysis of all HELEEOS engagement simulations is the HV 5/7.

Table 2 shows a comparison between Strehl ratios due to optical turbulence and thermal blooming, where a Strehl ratio of 1 indicates an absolute zero effect (i.e. no optical turbulence present) and a Strehl ratio close to zero indicates a maximum attenuation effect (i.e. the presence of very strong optical turbulence). In Table 2, the Strehl ratios due to optical turbulence are virtually identical in the presence and absence of aerosols. In the presence of the HV 5/7 optical turbulence profile, however, the Strehl ratio decreases from 0.991 (C_n^2=0 indicating no optical turbulence present) to 0.621 for the HV 5/7 profile. While the argument can be made that the presence of optical

turbulence does have an effect on a propagated laser beam (shown in the decrease in Strehl ratio due to optical turbulence), this effect is insignificant to the effect that thermal blooming has on a laser beam as indicated by the extremely low Strehl values due to thermal blooming in Table 2. As a result, the effect of optical turbulence on a propagated laser beam can be viewed as negligible, or ineffective, for ATL engagements as the slant ranges from platform to target become increasingly vertical.

Table 2. HELEEOS summer strehl ratios due to optical turbulence and thermal blooming for ATL engagements where the platform altitude is 5km and the target altitude is 0m. Maximum slant range is 15km and minimum slant range is approximately 8.7km for this engagement. The strehl ratios due to optical turbulence are virtually identical in the presence and absence of atmospheric aerosols. The strehl ratios due to optical turbulence decrease as the optical turbulence profile changes from the C_n^2=0 (i.e. no optical turbulence present) profile to the HV 5/7 standard profile. However, the decrease in strehl ratio due to optical turbulence is insignificant compared to the low strehl ratio values due to thermal blooming. The *strehl ratio (bottom row) indicates the effect of the HV 5/7 optical turbulence profile over a 5km slant range where the platform altitude is 100m and the target altitude is 0m; indicating a low, virtually horizontal, altitude geometry (representing realistic Army engagements).

HELEEOS Summer Strehl Ratios			
		Strehl Ratios due to Optical Turbulence	Strehl Ratios due to Thermal Blooming
Strehl ratio without GADS aerosols	C_n^2=0 (i.e. No optical turbulence present)	0.991	0.057
Strehl ratio without GADS aerosols	HV 5/7	0.621	0.079
Strehl ratio with GADS aerosols	C_n^2=0 (i.e. No optical turbulence present)	0.991	0.094
Strehl ratio with GADS aerosols	HV 5/7	0.622	0.128
*Strehl ratio with GADS aerosols	HV 5/7	0.006	0.476

As slant ranges from platform to target become increasingly horizontal and low in altitude, the effect of optical turbulence on a propagated laser beam increases significantly, even for smaller slant ranges relative to typical ATL slant ranges. This is indicated by the *Strehl ratio with GADS aerosols in Table 2, where the geometry for

this specific engagement consisted of a 5km slant range, a platform altitude of 100m, and a target altitude of 0m; representing a low altitude, virtually horizontal, engagement. Engagements such as these may be typical for Army engagements but are not really applicable to ATL engagements.

It is interesting to note that the Strehl ratios with thermal blooming improve slightly in the presence of turbulence and/or aerosols (see values in rightmost column of Tablee 2). In the case of aerosols, this is due to the extinction from aerosols being 90% due to scattering; scattering removes energy from the beam without heating it, thus reducing thermal blooming. Turbulence broadens the beam and therefore spreads the heating due to absorption over a larger volume; this also reduces thermal blooming.

Relative Humidity Effect on Irradiance

In testing the relative humidity (RH) effects, HELEEOS allows for a wide range of RH percentile values. Rather than run all possible RH percentile values, running five RH percentile values is sufficient for observing the effectiveness of RH at WPAFB on the target peak irradiance. In Figures 12 and 13, the maximum irradiance curve occurs for the 1^{st} percentile RH at WPAFB, OH. The minimum irradiance curve occurs for the 99^{th} percentile RH at WPAFB, OH, (assuming all other atmospheric weather conditions are the same with the exception of temperature, which changes with different RH percentiles). In knowing the profile of these two curves, one is able to determine the peak irradiance that is most and least likely to occur. Based on HELEEOS data for WPAFB, OH, Figures 12 and 13 identify the probability of effectiveness at WPAFB, OH in the summer and winter respectively.

Since water vapor has a tendency to absorb energy at the 1.315μm COIL wavelength, then it would only make sense that as the amount of moisture or water vapor increases in the atmosphere, then the amount of absorption due to the atmospheric moisture would also increase, thereby allowing less irradiance to transmit through the

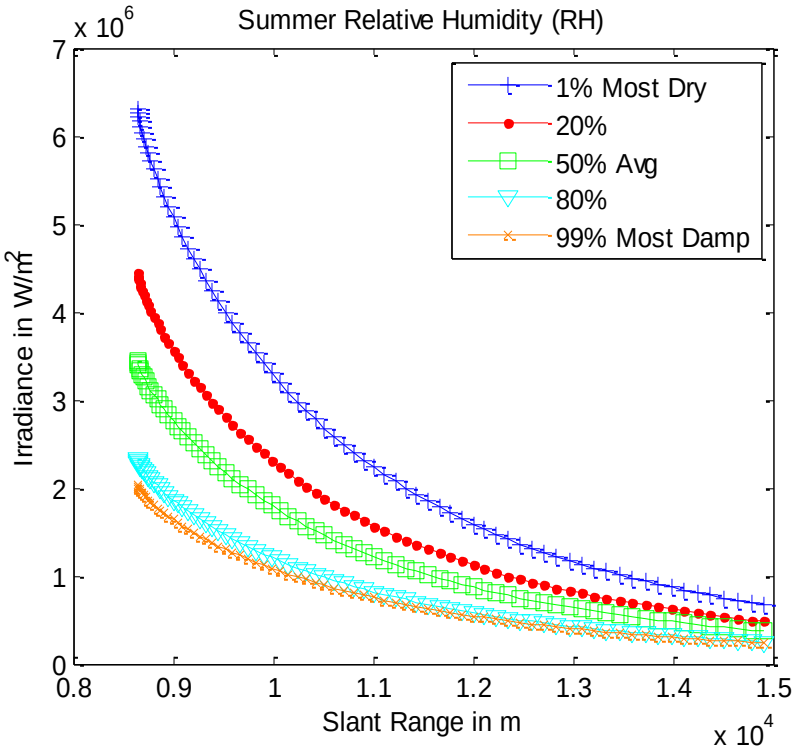

Figure 12. HELEEOS summer percentile RH. Curves shown illustrate the probability of resulting peak irradiance occurring at WPAFB during the summer. The peak irradiance output is based on recorded RH data for this specific geographical location. The greatest peak irradiance curve occurs in the 1st percentile RH. The lowest peak irradiance curve occurs in the 99th percentile RH for WPAFB. Since the data represent percentiles in a normal distribution, then the probability of the 1st percentile RH and a 99th percentile RH yield the least likely occurrences. Furthermore, a normal distribution implies that the best fit for testing is the 50th percentile, which is most likely to occur based on the data gathered at WPAFB, OH. The irradiance curves take into account the Global Aerosol Data Set for aerosol type and the HV 5/7 for the optical turbulence type.

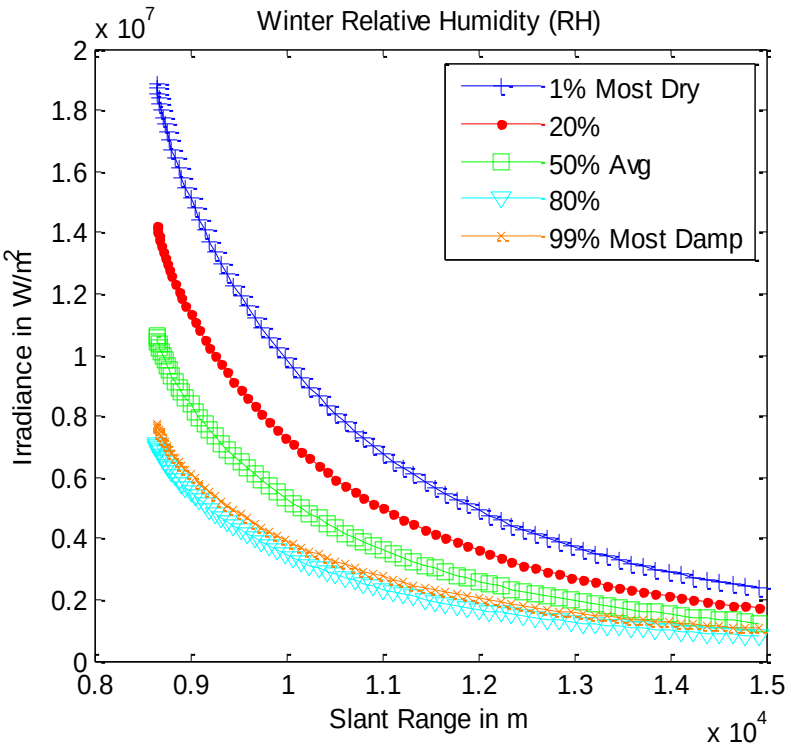

Figure 13. HELEEOS winter percentile RH. Curves shown illustrate the probability of resulting peak irradiance occurring at WPAFB during the winter. The peak irradiance output is based on recorded RH data for this specific geographical location. The greatest peak irradiance curve occurs in the 1st percentile RH. The lowest peak irradiance curve occurs in the 80th percentile RH for WPAFB. Since the data represent percentiles in a normal distribution, then the probability of the 1st percentile RH and a 99th percentile RH yield the least likely occurrences. Furthermore, a normal distribution implies that the best fit for testing is the 50th percentile, which is most likely to occur based on the data gathered at WPAFB, OH. Note that the 99th percentile curve slightly exceeds the 80th percentile curve. This is likely a result of the RH values being 100% or nearly that value for both the 99th and 80th percentiles, and higher temperatures being associated with the 80th percentile during the winter at WPAFB, OH. The irradiance curves take into account the Global Aerosol Data Set for aerosol type and the HV 5/7 for the optical turbulence type.

atmosphere and reach the target. In Figure 13, the percentile RH peak irradiance curves for the winter are significantly greater than in the summer (Figure 12). This assessment means the probability of effectiveness of the ATL at WPAFB, OH is greater in the winter than the summer. Furthermore, the amount of water vapor in the atmosphere is significantly greater in the summer than winter at this location. In the simulated engagements, choosing a percentile RH of 50% (average) is a best fit since a 50th

percentile, based on a normal probability distribution, represents the average most likely scenario.

Irradiance Dependence on Time of Day

In comparing the irradiance versus the time of day during the summer and winter (i.e. Figures 14 and 15), it is seen that the irradiance curves vary slightly for different times of day, however the variance is much greater from summer to winter. In the summer and winter time, the variance in irradiance curves is most likely a result in the interaction of the propagated laser beam with the atmospheric boundary layer. As mentioned in Chapter II, the boundary layer is the portion of the atmosphere that is most affected by the surface of the Earth, which can range from tens of meters to 4 km or more (Wallace and Hobbs, 2006). Since the boundary layer consists of that region of the atmosphere where turbulence is strongest and pollutants are at highest concentrations, it is reasonable to assume that a change in thickness of the boundary layer would result in a change in the irradiance on target (i.e. the effect of turbulence and pollutants on the propagated laser beam) as the laser beam propagates through the boundary layer. Typically this might allow for the assumption that the time of day in which the peak irradiance curve is greatest occurs from 0300-0600, implying the greatest amount of transmittance during this timeframe. This makes sense in accordance with the evolution of the BL in Chapter II. In addition, one might also assume that the time of day in which the peak irradiance curve is the lowest occurs from 1500-1800, implying that the lowest amount of transmittance occurs during this timeframe. Interestingly, this is not the case observed in Figures 14 and 15.

In Figure 14, the time of day yielding the greatest irradiance curve is from 0900-1200. In addition, the time of day yielding the lowest irradiance curve is from 0300-0600. The primary reason for this apparent discrepancy is the relationship between the BL and absolute humidity, relative humidity, and temperature.

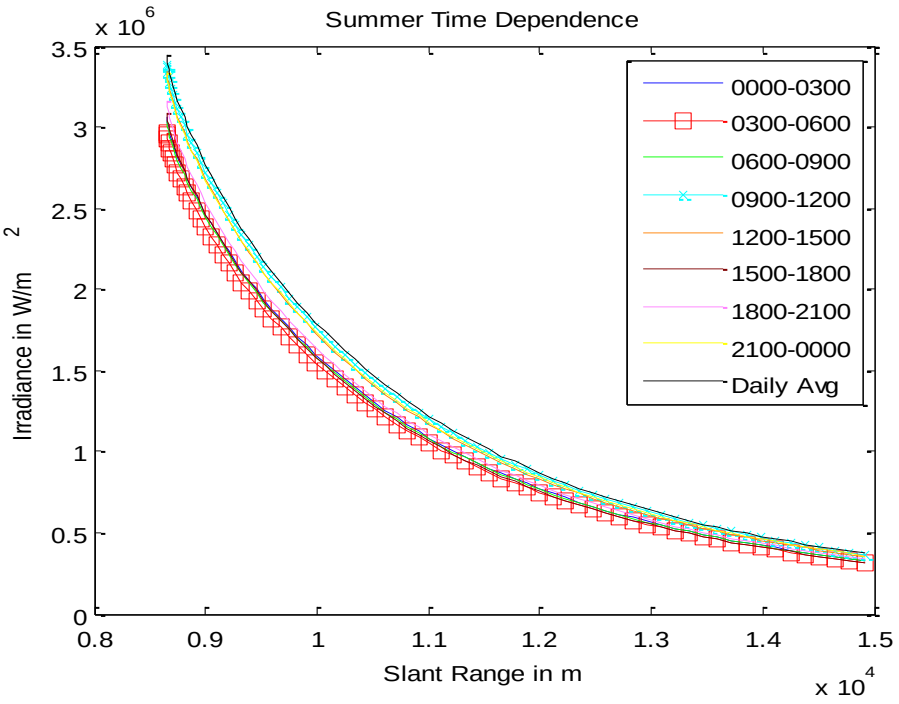

Figure 14. HELEEOS summer time of day dependence. Peak irradiance curves for various times of day at WPAFB during the summer. The greatest peak irradiance occurs between 0900-1200 (excluding the peak irradiance curve for the daily average). The lowest peak irradiance curve occurs between 0300-0600. The irradiance curves take into account the Global Aerosol Data Set for aerosol type and the HV 5/7 for the optical turbulence type.

A decrease in temperature within a given season results in an increase in RH, assuming the absolute humidity remains constant. Also note that temperature throughout the BL is defined by the surface temperature and decreases at the dry adiabatic lapse rate given by the following equation:

$$\left(\frac{dT}{dz}\right)_{dry} = -\frac{g}{c_p} = -9.8K \cdot km^{-1} \tag{15}$$

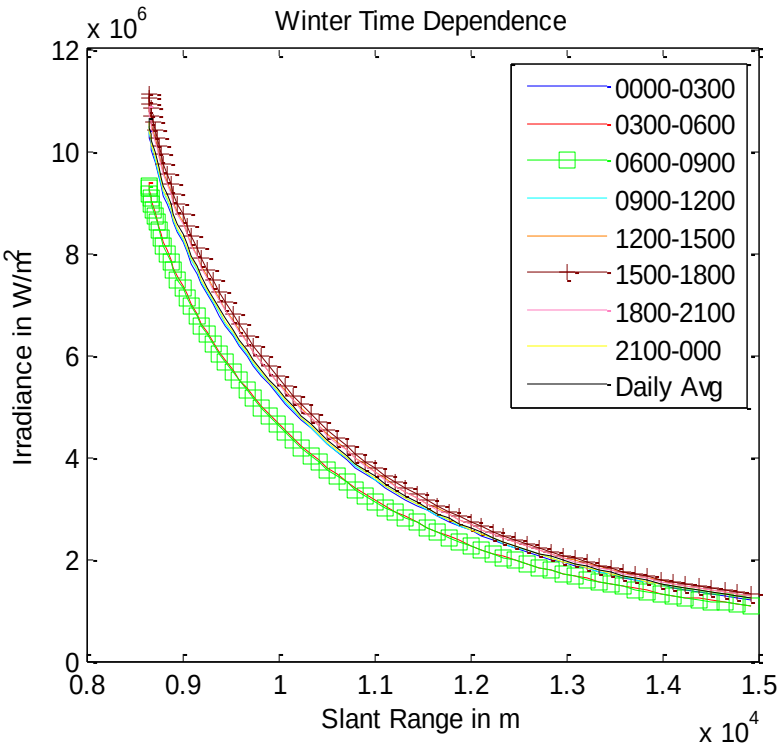

Figure 15. HELEEOS winter time of day dependence. Peak irradiance curves for various times of day at WPAFB during the summer. The greatest peak irradiance occurs between 1500-1800 (excluding the peak irradiance curve for the daily average). The lowest peak irradiance curve occurs between 0600-0900. The irradiance curves take into account the Global Aerosol Data Set for aerosol type and the HV 5/7 for the optical turbulence type.

Similarly, the dewpoint temperature, which is defined as the temperature at which saturation occurs in a volume of air when cooled at a constant pressure, also decreases at a lapse rate with height given by the following equation:

$$\left(\frac{dT_d}{dz}\right) = -\frac{g}{\varepsilon \cdot l_v} \cdot \frac{T_d^2}{T} \approx -1.8K \cdot km^{-1} \tag{16}$$

In the Equations 15 and 16, T is temperature(K), T_d is dewpoint temperature(K), z is height (m), g is the gravitational constant ($m \cdot s^{-2}$), c_p is the specific heat of air at constant pressure ($J \cdot kg^{-1} \cdot K^{-1}$), ε is the ratio of the molecular weight of water over the molecular weight of dry air, and l_v is the latent heat of the vaporization of water ($J \cdot kg^{-1}$). Comparing these two lapse rates, saturation can occur within the height of the BL because the temperature lapses at a rate much greater than the dewpoint temperature. It is important to note that the HELEEOS model allows these lapse rates to occur when using ExPERT sites (Extreme and Percentile Environmental Reference Tables) such as Wright-Patterson Air Force Base (WPAFB)/Dayton, Ohio, which was the site used for every test in this research. In addition, a consequence of these lapse rates is that the RH varies dramatically within the BL, increasing to 100% in most cases. Due to the RH-driven water uptake by water-soluble aerosols, predominantly found in mid-latitude sites such as WPAFB, the increase in RH from the surface through the BL has a strong effect on the aerosol size distribution, which in turn affects simulated laser propagation (Fiorino et al, 2007). Ultimately, the height of the BL over land that is used in the HELEEOS model, shown in Table 3, helps explain the reason the greatest irradiance curve occurs during the 0900-1200 timeframe in the summer while the lowest irradiance curve occurs from 0300-0600. In Table 3, the BL is the thinnest from 0000-0600. This would imply a high RH resulting from the decrease in temperature throughout the nocturnal timeframe, which in turn implies saturated or near saturated conditions and a larger size distribution of water-soluble aerosols in the BL (Fiorino et al, 2005). Since 0300-0600 is the timeframe just before the RH begins to decrease due to the rising temperatures that come with sunrise, then the reason the irradiance curve is lowest during this timeframe is because of the

amount of water molecules adhering to the water-soluble aerosols. Conversely, during the timeframe of 0900 to 1200, the BL has just reached its greatest depth. This means that the RH has dramatically decreased due to the rising temperatures throughout the morning. As a result, the aerosol size distribution, which is driven by RH, and dew points are near a minimum. This yields an overall low absorption and the greatest peak irradiance during this timeframe (Fiorino, 2008). Similarly, in the winter, the timeframe just before the BL starts to increase above its lowest level implies the highest RH in the atmosphere, which results in the lowest peak irradiance occurring from 0600-0900; and the greatest irradiance occurring from 1500-1800, due to the lowest RH in the atmosphere at WPAFB, OH.

Table 3. Overland Boundary Layer Height (in meters) as a function of season and time of day. Notice the BL reaches maximum thickness at 0900. Conversely, from 0300-0600 the BL is at a minimum thickness for the greatest amount of time.

Time of Day (Local)	Summer	Winter
0000-0259	500	500
0300-0559	500	500
0600-0859	1000	500
0900-1159	1524	1000
1200-1459	1524	1524
1500-1759	1524	1524
1800-2059	1524	1000
2100-2359	1000	500

As mentioned in Chapter II, winter nights are longer than the day, which means that the stable boundary layer that occurs in the evening is much thicker in the winter than in the summer. In addition, the turbulent mixing layer that forms during the day is lower in the winter than in the summer, which means that there is less of an effect on the propagated laser beam by the boundary layer in the winter than in the summer. Since the irradiance curves vary slightly within each season, it is sufficient to choose a daily

average timeframe for the analysis of HELEEOS simulation engagements. This, however, does not mean that the daily average timeframe is used for every real-world engagement. Figures 14 and 15 illustrate differences in the effectiveness of the ATL COIL between summer and winter as well as certain timeframes during the day.

Aerosol Effects on Irradiance

As mentioned in Chapter II, aerosols are defined as small solid and/or liquid suspended particles (not including cloud droplets) and are able to stay suspended due to their negligible terminal velocities. Figures 16 and 17 illustrate the aerosol effects by a variety of aerosol types. The Global Aerosol Data Set (GADS) profile, which overlaps the Continental Average aerosol profile, provides a good fit for testing purposes since the GADS profile takes into account aerosol constituent number densities on a 5° by 5° worldwide grid (Koepke et al, 1997). In addition, the GADS profile is a good fit as seen by the overlapping of the Continental Average aerosol profile, which is an aerosol profile used to describe continental areas containing soot and an increased amount of insoluble and water-soluble components (Hess et al, 1998) commonly found in mid-latitude geographical locations such as WPAFB/Dayton, OH. In addition, the GADS profile virtually bisects the Continental Clean and Continental Polluted aerosol profiles, which represent the two extreme continental areas containing very low and high anthropogenic influences, respectively. This observation reinforces the fact that the GADS profile is a good representation of the aerosol content for mid-latitude areas such as WPAFB, OH.

There is a significant increase of transmittance from summer to winter, which is based on the increase (by approximately a factor of 4) of peak irradiance curves from summer to winter seen in Figures 16 and 17. The reason for this occurrence is consistent

in the relationship with temperature, absolute humidity, and aerosol number density in the BL.

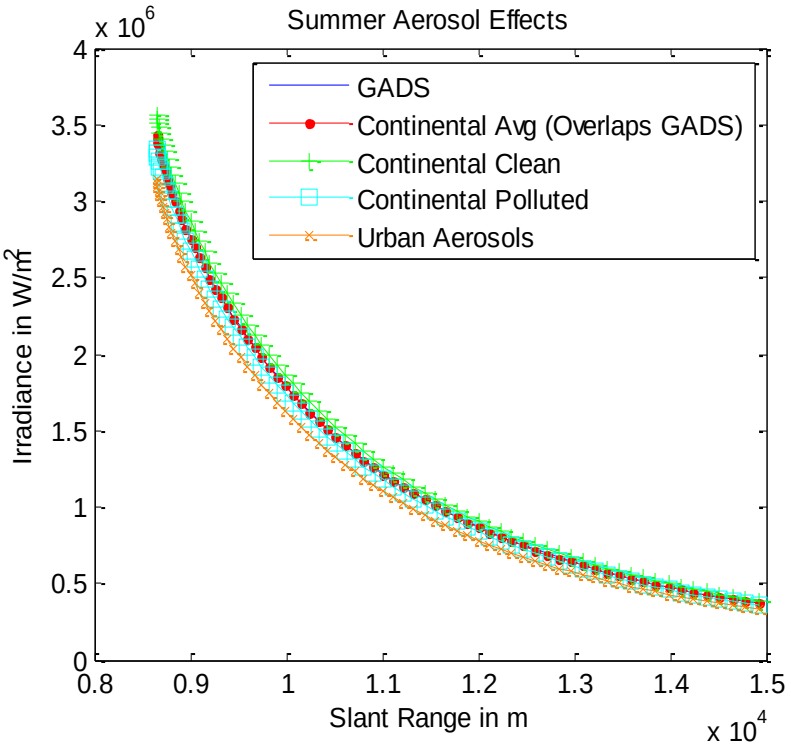

Figure 16. HELEEOS summer aerosol profile effects. Peak irradiance curves are based on the aerosol mixture for WPAFB in the summer. The greatest peak irradiance occurs for the Continental Clean profile. The lowest peak irradiance occurs for the Urban Aerosols profile. The peak irradiance curve for the GADS profile bisects the Continental Clean and Urban Aerosols profiles.

In comparing the curves in Figures 16 and 17 back to the 50th percentile curves in Figures 12 and 13, one can see that the effects of aerosols is significantly smaller than the relative humidity effect. This is because the relative humidity percentiles shown in Figures 12 and 13 are tied strongly to the absolute humidity, which is generally higher in the summer than the winter due to a greater amount of evaporation resulting from higher temperatures, thus causing greater absorption of the 1.315μm ATL beam.

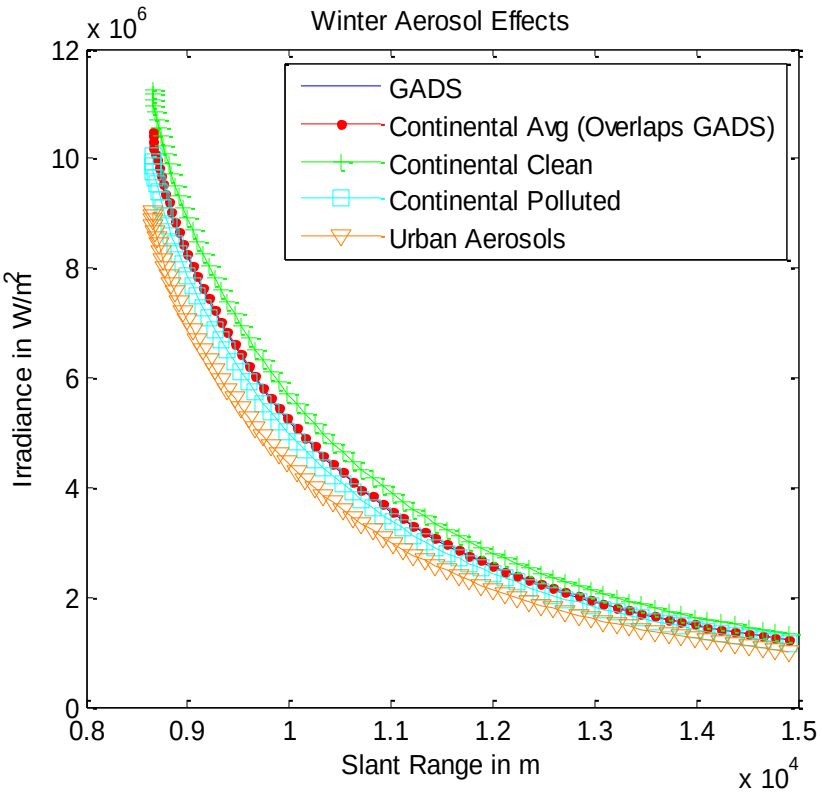

Figure 17. HELEEOS winter aerosol profile effects. Peak irradiance curves are based on the aerosol mixture for WPAFB in the winter, which may vary from the summer. The greatest peak irradiance occurs for the Continental Clean profile. The lowest peak irradiance occurs for the Urban Aerosols profile. The peak irradiance curve for the GADS profile bisects the Continental Clean and Urban Aerosols profiles.

The water-soluble aerosols commonly found in mid-latitude regions do in fact increase in size and scatter more energy with higher relative humidity. This means that there is actually more aerosol scattering in the winter than in the summer because relative humidity is usually higher in the winter due to lower temperatures. However, this effect is not clearly discernible in the at the COIL wavelength in the figures shown in this research due to the strong water vapor absorption at low altitudes.

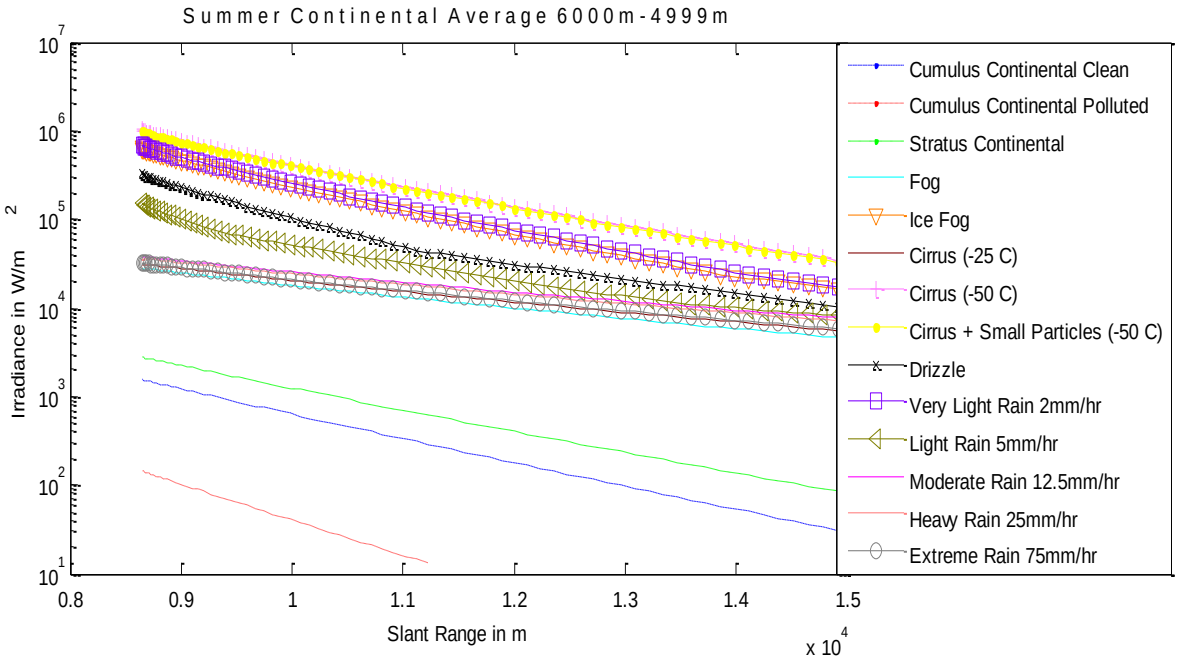

Figure 18. HELEEOS summer 1 meter depth cloud and rain (Logarithmic Scale). Peak irradiance curves for various cloud or rain condition. Since the altitude of the aircraft is 5000m and the cloud or rain condition ranges from 6000m-4999m, the laser beam propagates through 1 meter of cloud or rain. As effective radius (r_{eff}) decreases and number particle density (N) increases, the transmission of the laser beam decreases (Table 1b, Hess et al, 1998). Significant transmission occurs for Ice Fog, Cirrus (-50 C), Cirrus (-50 C) + Small Particles, Drizzle, Very Light Rain, and Light Rain. All others result in negligible peak irradiance. The irradiance curves take into account the Global Aerosol Data Set for aerosol type.

Cloud and Rain Effects on Irradiance

In Figures 18-20, the effects that clouds and rain have on peak irradiance of a propagated laser beam during the summer and winter seasons are shown. Figure 18 shows strong differences in the type of cloud or rain conditions through which the laser beam propagates. For this case, the target is stationary and is approached by the aircraft at a constant horizontal velocity.

The irradiance curves in Figure 18 can be segregated into three groups. The first group includes the cloud and rain conditions that produce the optimum peak irradiance on target. Notice that the condition for optimum irradiance is the Cirrus (-50°C) followed

closely by Cirrus (-50°C) with small particles. In addition, the next two conditions that yield the next best irradiance curves are the very light rain (2mm·hr^{-1}) and ice fog conditions, which are then followed by drizzle and light rain (5mm·hr^{-1}). This decrease in irradiance is directly related to the relationship that exists with the extinction, effective radius r_{eff}, and number density of particles in a polydisperse cloud or rain condition. Note that the effective radius is a result of a polydisperse cloud or rain condition, in which the particle radii are non-uniform, unlike a monodisperse cloud where all particle radii are equal. The relationship is best described using the following equation (Petty, 2006):

$$\beta_e = k_e \cdot \rho_w \tag{17}$$

Where β_e is the total extinction coefficient, k_e is the mass extinction coefficient given by the following equation (Petty, 2006):

$$k_e = \frac{3Q_e}{4\rho_l r} \tag{18}$$

with Q_e (extinction efficiency)≈2 for large particles, ρ_l (pure water density)≈1000kg·m^{-3} and ρ_w is the local cloud or rain water density per unit volume of air given by the following equation (Petty, 2006):

$$\rho_w = N\frac{4}{3}\pi r^3 \rho_l \tag{19}$$

Furthermore, Equation 17 can be written in terms of r_{eff} to look like the following equation (Petty, 2006):

$$\beta_e \approx \frac{3\rho_w}{2\rho_l \cdot r_{eff}} \tag{20}$$

The important thing to notice in Equation 20 is that the total extinction is dependent on the effective radius r_{eff} and the number density N (via Equations 19 and 20), which is directly proportional to the local cloud or rain water density per unit volume of air ρ_w. This relationship is important because as the value of N increases (i.e. ρ_w increases), the total extinction increases. Similarly, as the value of r_{eff} decreases, the total extinction also increases. Since the HELEEOS model uses cloud and rain conditions that are characterized and defined by the Optical Properties of Aerosol and Clouds (OPAC) code (Fiorino et al, 2007), then from the Hess et al (1998) OPAC code, as N increases and r_{eff} decreases; as represented by a change in cloud condition from Cirrus (-50°C) to Cirrus (-50°C) + small particles. This means that the total extinction must increase from Cirrus (-50°C) to Cirrus (-50°C) + small particles, thereby causing a decrease in irradiance. Comparing this trend with all of the other cloud and rain conditions, the increases in number density N and the decreases in effective radius r_{eff} are the primary reasons that the extinction increases, which results in the optimum irradiance curve for the Cirrus (-50°C) cloud condition and the least amount of irradiance for the Cumulus Continental Polluted cloud condition.

In Figures 18-20, the effect of the depth of the cloud or rain condition has on irradiance is shown. The depth of the cloud or rain condition varies from 1m, 50m, to 500m in these three figures, respectively, in order to illustrate the effects that the changes in optical path, which is briefly defined in Chapter II, has on irradiance. For the cases of cloud and rain conditions, the optical path that is most critical is the path that the laser beam takes from the aperture (i.e. the aircraft platform) to the exit point of the specific cloud or rain depth. The relationship between optical path and total extinction is best described by the following equation:

$$t(s_1, s_2) \equiv e^{\int_{s1}^{s_2} \beta_e(s)\, ds} \tag{21}$$

Where t is transmittance described in Chapter II, and s_1 and s_2 are the start and ending points of the optical path of the laser beam within the thickness of the cloud or rain condition. As the distance from s_1 to s_2 increases, the integral in the exponent in Equation 21 also increases, which means that the total transmittance value t decreases due to the negative sign in the exponent.

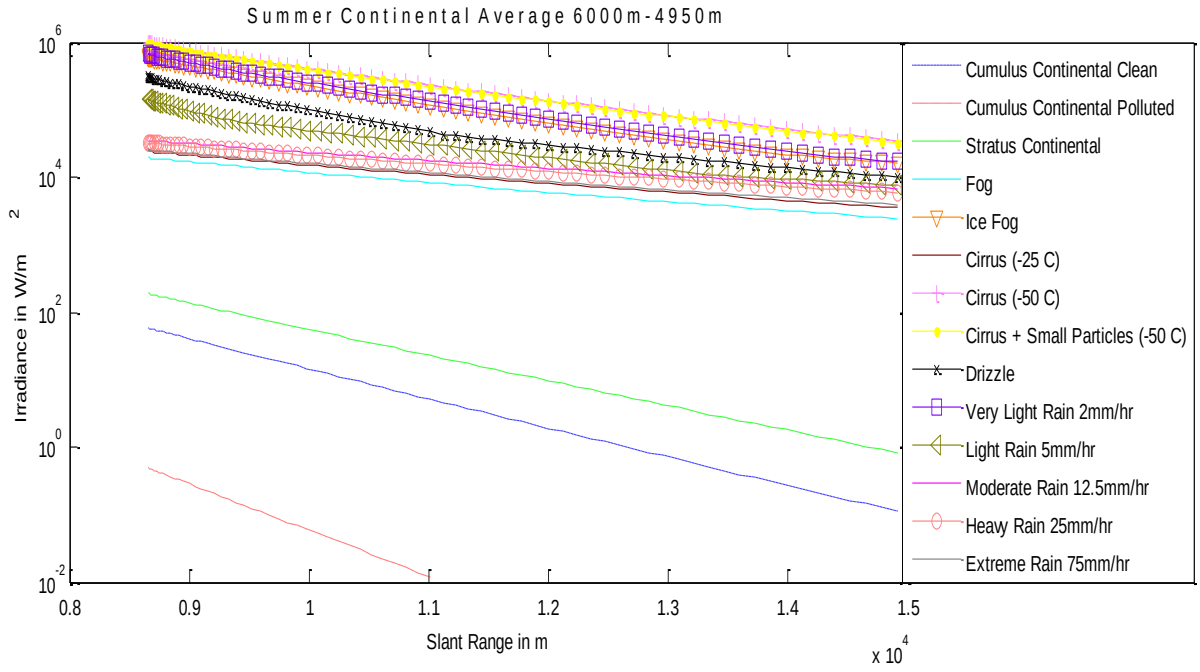

Figure 19. HELEEOS summer 50 meter depth cloud and rain (Logarithmic Scale). Peak irradiance curves for various cloud or rain condition. Since the altitude of the aircraft is 5000m and the cloud or rain condition ranges from 6000m-4950m, the laser beam propagates through 50 meters of cloud or rain. As effective radius (r_{eff}) decreases and number particle density (N) increases, the transmission of the laser beam decreases (Table 1b, Hess et al, 1998). Significant transmission occurs for Ice Fog, Cirrus (-50 C), Cirrus (-50 C) + Small Particles, Drizzle, Very Light Rain, and Light Rain. All others result in negligible peak irradiance. The irradiance curves take into account the Global Aerosol Data Set for aerosol type.

As per the description of transmittance in Chapter II, a larger value (ranging from 0 to 1) means less attenuation. Therefore, we can see that as the layer of cloud or rain condition increases beneath the platform, the optical path in which the laser beam propagates through the condition also increases and causes less transmittance, or more attenuation, of the laser beam. This result is the reason the peak irradiance curves decrease as the cloud or rain depth increases beneath the platform.

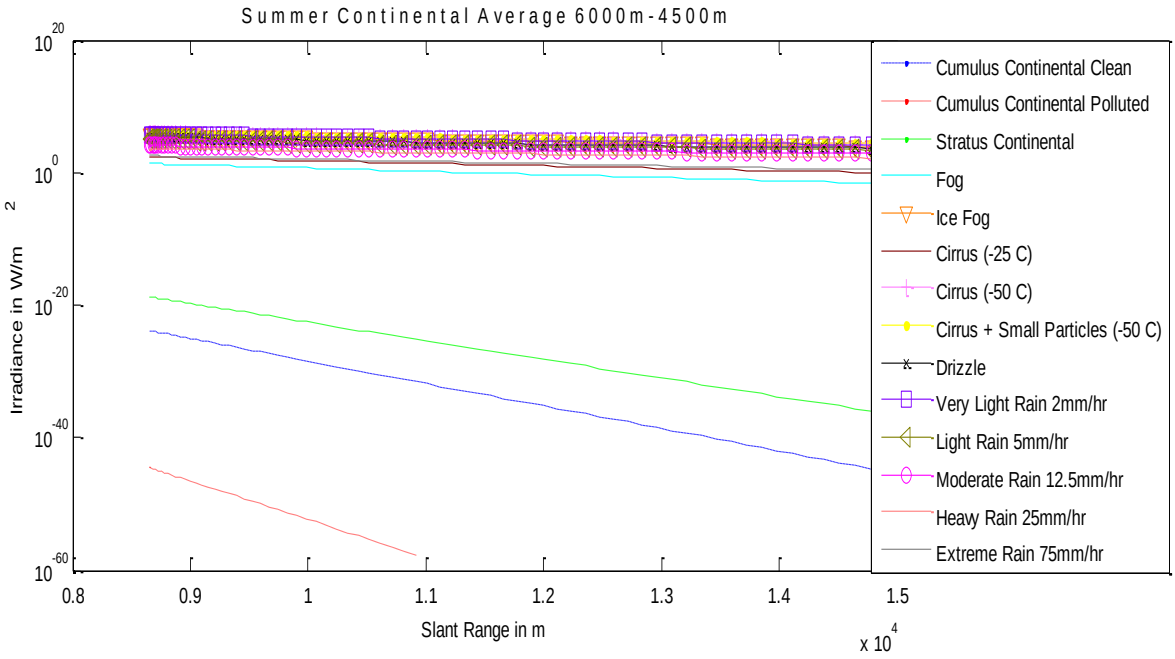

Figure 20. HELEEOS summer 500 meter depth cloud and rain (Logarithmic Scale). Peak irradiance curves for various cloud or rain condition. Since the altitude of the aircraft is 5000m and the cloud or rain condition ranges from 6000m-4500m, the laser beam propagates through 500 meters of cloud or rain. As effective radius (r_{eff}) decreases and number particle density (N) increases, the transmission of the laser beam decreases (Table 1b, Hess et al, 1998). Significant transmission occurs for Ice Fog, Cirrus (-50 C), Cirrus (-50 C) + Small Particles, Drizzle, Very Light Rain, and Light Rain. All others result in negligible peak irradiance. The irradiance curves take into account the Global Aerosol Data Set for aerosol type.

Thermal Blooming: Dynamic Platform to Stationary v. Dynamic Target

In Figure 21, the effect of a dynamic platform approaching a stationary target versus a dynamic target is shown during the winter. One observation is that the irradiance on target is optimal when the platform is moving in the same direction as the target (i.e. the platform is engaged on a target as the platform approaches the target from behind). In addition, a second observation is that a dynamic target that is moving in the opposite direction as the platform (i.e. platform to target relative azimuth angle is 0˚ and target heading is 180˚) will initially have a greater irradiance on target than if the target were stationary. The irradiance, however, does not increase at the same rate for a

decreasing slant range as it would if the target were stationary. As a result, the irradiance on target becomes less effective for the case of an approaching target than one that is stationary as the platform flies within a certain slant range.

In Figure 21, a target moving southbound at $10 m \cdot s^{-1}$ (while the platform moves northbound at $50 m \cdot s^{-1}$) results in a greater peak irradiance on target than if the target were stationary at a slant range of 15km or less. This remains true until the platform decreases the slant range to approximately 10.8km. At this point, the irradiance on target is no longer greater than if the target were stationary. In fact, the irradiance on target becomes less at closer slant ranges and is therefore less efficient than if the target were stationary. This is the result of the thermal blooming effect defined in Chapter II. As discussed before, a stationary laser beam results in a larger amount of thermal blooming due to the fact that the laser beam is constantly heating the same propagation path, thereby causing the laser beam to diverge more than usual and result in less irradiance on target. For the case of the target moving in the same direction as the platform (i.e. platform and target both travel northbound), the laser beam is always in motion at every point along the propagation path and never heats any part of the propagation path for very long.

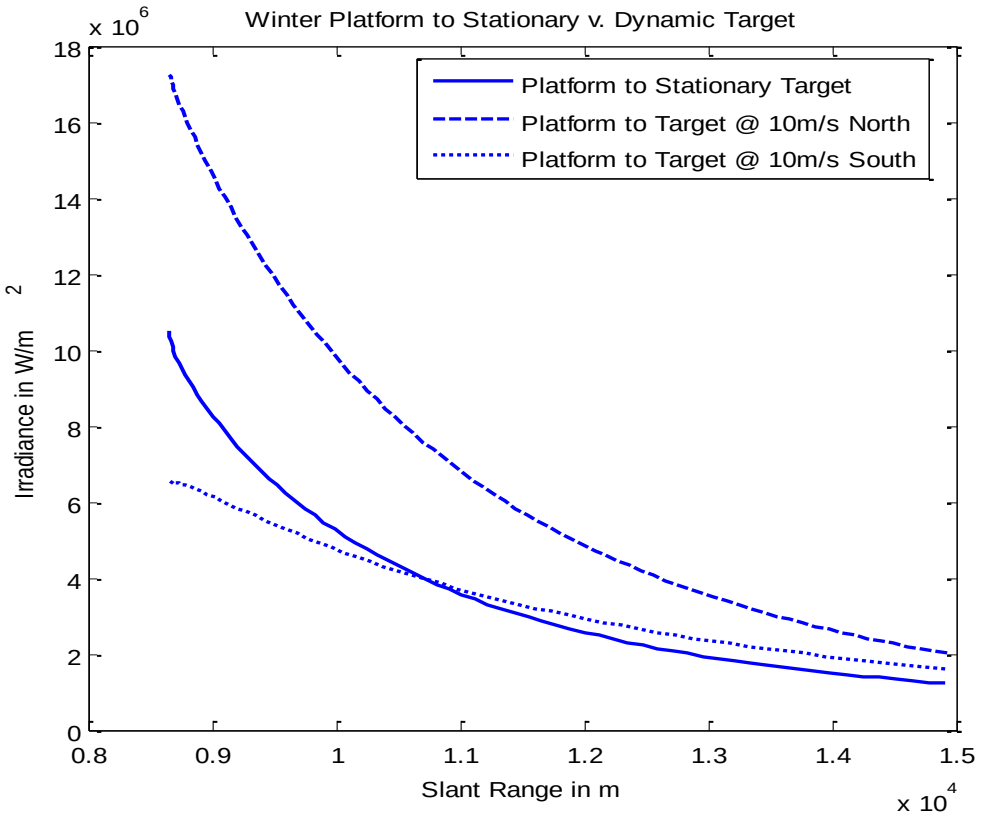

Figure 21. HELEEOS winter thermal blooming effects. Aircraft is northbound with a velocity of 50m·s^{-1}. Peak irradiance curve is greatest when the platform and target move in the same direction. Peak irradiance curves for platform to stationary and southbound target intersect at a specific slant range due changes in thermal blooming effects. Within that specific slant range (occurring at approximately 10.75km in the figure) the peak irradiance becomes less for the southbound than the stationary target due to greater thermal blooming effects. There are no clouds or rain present during this engagement.

For the case of the stationary target, however, the laser beam moves slower at points along the propagation path that is closest to the target. This means that the propagation path closest to the target heats up the most and therefore creates more thermal blooming than the case of the northbound target, causing less irradiance on target for all slant ranges. For the case of the target moving in the opposite direction as the platform (i.e. platform travels north and target travels south, where the target initial relative azimuth angle is 0˚), the laser beam is constantly in motion much like the case for

the northbound target. However, for the southbound target, as the target approaches the platform, there is a point along the beam path that is seemingly idle, where the height of this idle point depends on the difference in velocities between the platform and the target. One way to look at this is to theoretically imagine the platform and target traveling at equal but opposite velocities, which would result in the idle point of the laser beam to occur at exactly half the distance between the platform and the target. In addition, a greater platform speed than target speed (i.e. a most probable case) causes the most heating at points closest to the target. Conversely, a greater target speed than platform speed (i.e. a highly unlikely case) causes the most heating to occur at points closest to the platform. Since a diverging laser beam is less effective as it propagates over a distance, having the idle point of the laser beam occur as close to the target as possible results in the least amount of beam spread and, therefore, maximum effectiveness.

Figure 21 illustrates the northbound platform to southbound target case such that as the platform to target slant range decreases (i.e. the platform gets closer to the target), the amount of divergence caused by the propagation path increasing in temperature becomes closer to that of the case of the stationary target, eventually causing an overall equal amount of thermal blooming effect on the laser beam for both cases. As the slant range decreases, the height at which the laser beam begins to diverge as a result of thermal blooming continues to increase and results in a greater amount of divergence, exceeding the amount of thermal blooming for the case of the stationary target. This is primarily the reason the peak irradiance curve of the southbound target engagement starts greater but eventually becomes less than the stationary target engagement as the platform to target slant range decreases in the winter at WPAFB, OH.

Figure 22 illustrates the thermal blooming effects in the summer. Unlike the winter engagements shown in Figure 21, the northbound platform to southbound target engagement irradiance curve begins slightly less than the stationary engagement irradiance curve and gradually becomes more ineffective as the slant range from platform to target decreases. This is primarily a result of a greater absolute humidity in the summer than winter at WPAFB, OH, shown in Figure 23. A greater absolute humidity means that there is more atmospheric absorption and therefore an increase in temperature and thermal blooming of the laser beam. Since thermal blooming is a non-linear effect, an increase in thermal blooming results in a greater magnitude of attenuation for larger slant ranges. In the summer, the northbound platform to southbound target engagement experiences the most attenuation due to thermal blooming for all slant ranges; the northbound platform to northbound target engagement experiences the least amount of attenuation, illustrating the optimal engagement condition for all slant ranges.

Thermal blooming is a non-linear effect dependent on the amount of atmospheric absorption and resultant heating along the propagation path. The non-linear effects of the heating can be significantly reduced if the amount of energy in the beam is reduced, perhaps through scattering photons out of the beam without an increase in absorption. Thus a change in the amount of scattering results in a change in thermal blooming, even if the absorption remains constant. It is critical to investigate the effect of this tradeoff to understand the optimal conditions for specific atmospheric environments such as WPAFB, OH.

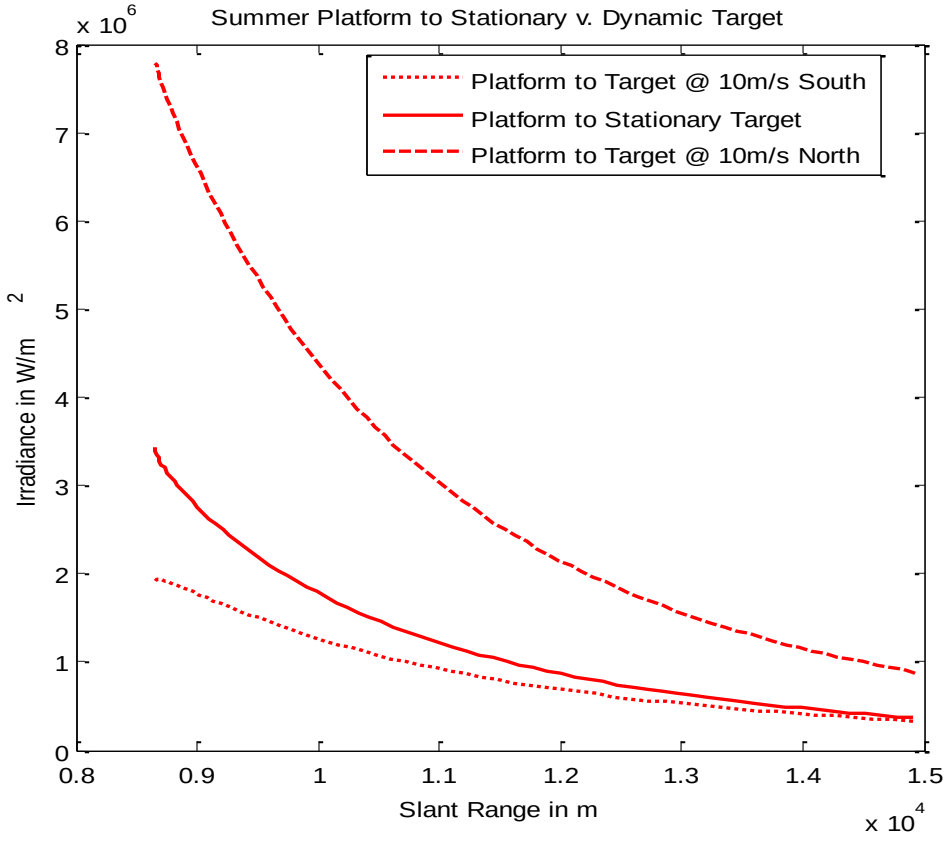

Figure 22. Simulated HELEEOS summer thermal blooming effects at WPAFB, OH. Aircraft is northbound with a velocity of 50m·s^{-1}. Peak irradiance curve is greatest when the platform and target move in the same direction. Peak irradiance curves for platform to stationary and southbound target do not intersect, unlike the winter case. Since absolute humidity is greater in the summer than winter, the propagation path experiences more absorption of light energy and is therefore heated to greater temperatures; causing a greater amount of divergence (beam spread) and thermal blooming. As a result, the irradiance curves for all three engagements are noticeably less than the irradiance curves for the winter engagements in Figure 21. There are no clouds or rain present during this engagement.

Figure 23 shows a greater absolute humidity in the summer than in the winter. Since water vapor acts as a natural absorber of the ATL wavelength (1.31525μm), there is a greater amount of absorption and thermal blooming in the summer than in the winter. Table 4 shows the change in path transmittance, peak irradiance, and power in bucket as the atmospheric visibility changes. For simulated summer engagements, the transmittance increases from 0.035741 to 0.63341 (where a value of 1 means complete

transmittance and 0 means absolutely no transmittance of the laser beam) as the visibility increases from 5km to 100km.

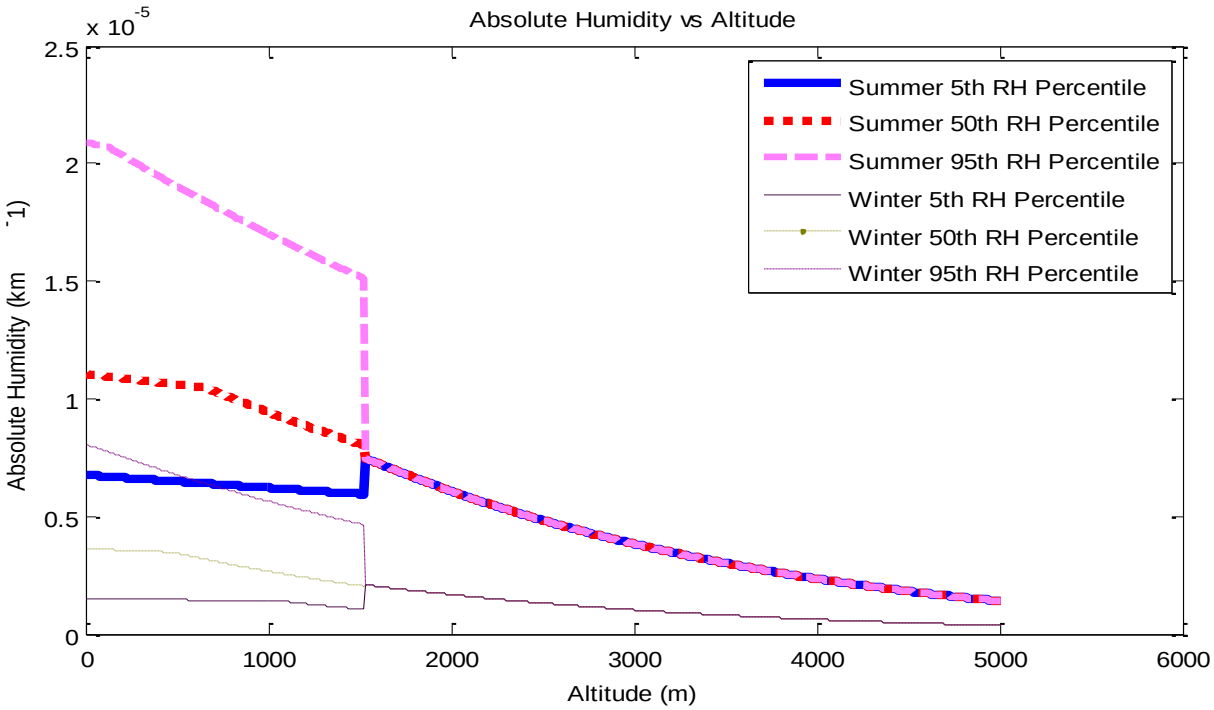

Figure 23. Absolute humidity for various RH percentiles in summer and winter at WPAFB, OH. The 50th percentile for summer shows greater absolute humidity within and above the boundary layer than the 50th RH percentile for the winter. This data was taken for daily average time of day, GADS aerosols, and HV 5/7 optical turbulence profiles.

This trend is consistent with the fact that an increase in visibility means a decrease in scattering due to aerosols. As a result, a reduction in scattering means that more of the laser beam is able to propagate without being redirected by the aerosols in the atmosphere. This means that there should be more light energy reaching the target as the transmittance increases, thereby resulting in an increase in peak irradiance and power in bucket as the visibility increases and scattering decreases. In the simulated engagements shown in Table 4, it is evident that the peak irradiance and power in bucket do in fact

increase as the visibility increases from 5km to 23km. However, as the visibility increases from 23km to 100km, the peak irradiance and power in bucket begin to decrease, implying an increase in attenuation in spite of the fact that scattering is decreasing. As scattering gradually decreases, the absorption along the propagation path gradually increases, which directly leads to an increase in thermal blooming.

Table 4. Summer versus winter path transmittance, all effects peak irradiance, and all effects power in bucket values that depend on varying visibilities. An increase in visibility means a decrease in scattering due to atmospheric aerosols. The all effects peak irradiance and power in bucket values shown are the values at the target at the initial slant range, 15km for these simulations. For the summer engagements shown, the optimal condition for laser propagation is when the visibility is 23km. The time of day used is daily average with an optical turbulence profile of HV 5/7 and GADS atmospheric aerosol profile.

50% RH (%-tile)	**Summer**			**Winter**		
Visibility	Path Transmittance	Peak Irradiance All Effects ($W \cdot m^{-2}$)	Power in Bucket All Effects (W)	Path Transmittance	Peak Irradiance All Effects ($W \cdot m^{-2}$)	Power in Bucket All Effects(W)
5km	0.035741	3.752366 E5	7.3251 E2	0.038307	4.844526 E5	9.116033 E2
10km	0.15134	6.779196 E5	1.405375 E3	0.179	1.325374 E6	2.651486 E3
23km	0.37003	8.0137 E5	1.729161 E3	0.46293	2.3161 E6	4.764034 E3
50km	0.5392	7.973449 E5	1.705487 E3	0.69154	2.910666 E6	6.040092 E3
100km	0.63341	7.674505 E5	1.674295 E3	0.82107	3.185425 E6	6.634929 E3

Because thermal blooming is a non-linear effect and scattering is a linear effect, the overall thermal blooming effect is able to eventually overcome the benefits in the decrease in scattering, which is evident in the simulated summer engagements in Table 4. Conversely, for winter engagements, the thermal blooming effect never overcomes the benefits in the decrease in scattering, resulting in a continuous increase in peak irradiance and power in bucket at the target as the visibility continues to increase. The primary reason for this is because of the fact that the absolute humidity is considerably less in the winter than in the summer at WPAFB, OH, as shown in Figure 23. Since the absolute

humidity is less in the winter, there are less water molecules in the atmosphere to absorb the light energy from the laser beam as it propagates, thereby resulting in an insufficient amount of thermal blooming to overcome the gain in laser beam performance resulting from the decrease in scattering. This observation not only proves that there is a tradeoff between scattering and thermal blooming, it proves that there exists a certain level of scattering and thermal blooming that optimizes the performance of the laser beam as it propagates through the atmosphere.

V. Conclusions and Recommendations

Conclusions

The research conducted in this thesis has shown that seasonal and time of day weather effects on BL HEL engagements are significant enough for the need of a HELTDA. The characterization of atmospheric and weather factors in the lower troposphere is essential in understanding and optimizing ATL engagements. The data gathered demonstrates the need to understand these parameters and the importance in determining the effectiveness of the ATL at WPAFB, OH.

The analysis of the data gathered in this document shows that there are ways to optimize the effectiveness and efficiency of ATL engagements. These optimal conditions should be sought and exploited whenever possible. By utilizing a HELTDA based on the HELEEOS software package, the war-fighter would likely be able to input certain atmospheric and weather conditions and determine an engagement plan in order to maximize effectiveness from the output data. It is important to understand that the analysis and results of this research only scratches the surface in the application in ATL engagements. The war-fighter must understand that there are many cases that can be tested in which the optimal results may differ. In principle, however, the results from this research may be applied to other cases in order to understand the reasons behind these differences. The results are as follows:

1. Optical turbulence is not a significant attenuating factor for currently envisioned ATL engagements.

2. Engagements in dryer climates are more effective than moist humid climates. ATL engagements in warm, humid, tropical locations will be less effective than locations that are cold and dry environments. This primarily is due to the fact that water vapor absorbs the 1.31525μm energy used by the ATL.

3. The effectiveness of the ATL decreases as the aerosol concentration increases (i.e. visibility decreases) with soot and water-soluble constituents. Optimal aerosol environments will be in remote warm, dry (i.e. low absolute humidity) continental areas that are removed from anthropogenic influences such as man-made pollution.

4. Optimal time of day engagements depend on the behavior and evolution of the BL at each geographical location before sunrise and sunset. For WPAFB, the optimal time of day for ATL engagements occurs between 0900-1200 in the summer and 1500-1800 in the winter.

5. For cloud and rain conditions, the optimal condition occurs for larger particle sizes with smaller concentrations per unit volume of air. Since Cirrus clouds have the largest particles and the lowest concentration per unit volume of air at -50˚ C, they are the cloud condition that yields the best results. However, Cirrus clouds occur at altitudes of approximately 6km, which is greater than the ATL operates. At WPAFB, OH, it is shown that the ATL maintains effectiveness for the cloud and rain conditions of very light rain, ice fog (albeit very unlikely at WPAFB), and drizzle.

6. The assessment of thermal blooming results in optimum effectiveness for engagements such that the target is traveling away from the platform and at a different altitude than the platform.

7. There is a tradeoff between thermal blooming and scattering. By increasing the amount of scattering along the propagation path, the amount of absorption by the water vapor in the atmosphere decreases. The amount of thermal blooming decreases since thermal blooming depends on absorption. Since thermal blooming attenuates non-linearly and extinction attenuates linearly, a change in thermal blooming attenuates to a larger degree than scattering.

Recommendations

As mentioned earlier, the results from this research only scratch the surface of the many cases that exist in ATL engagements in the lower troposphere. The fact is that there are still many factors that can be explored in determining the effectiveness of ATL engagements. Some recommendations for future research regarding the development of a HELTDA are as follows:

1. Consider various geographical locations. The results from this research are for the geographic location of WPAFB/Dayton, OH. Considering other geographic

locations will be beneficial in understanding the weather and atmospheric constituents that apply exclusively to that specific location.

2. Wind directions should also be factored. Wind velocities were not considered in this research due to time constraints. Understanding the wind velocity effects and relative wind velocity effects can be critical in understanding the relationship that wind velocities have on attenuating factors such as thermal blooming.

3. Not all aerosol profiles were explored in this research. Observing the effects of other aerosol environments may be necessary in determining the effects that other aerosols may have in combination with other atmospheric parameters.

4. Thermal blooming in certain cloud and rain conditions should be explored. In this research, thermal blooming was explored only for cases where cloud and rain were nonexistent. The effects that cloud and rain conditions have on thermal blooming are likely to be significant enough for future research.

5. The thermal blooming effects resulting from platform to stationary versus dynamic targets should be explored to a much greater extent. There are many combinations that can be tested in dynamic target engagements. In this research, the dynamic conditions that were tested only consisted of a target moving toward and away from the platform. There are many engagement angles that can be compared and tested to determine sufficient effectiveness and success in destroying stationary and dynamic targets.

6. Geometry of the aircraft-to-target engagement needs to be explored in more depth. The attenuation that the ATL experiences from turbulence is negligible for increasingly vertical engagements. As the engagements become increasingly oblique, the propagated beam encounters the parts of the atmosphere that are most turbulent for greater distances. This trade off in turbulence versus slant angle should also be explored for efficiency possibilities.

Bibliography

Bartell, R. J. (2008). Personal communication on November 18, 2008.

Fiorino, S. T. (2008). Personal communication on November 11, 2008.

Fiorino, S. T., Bartell, R. J., Krizo, M. J., & Cusumano, S. J. (2007). *Expected Worldwide, Low-Altitude Laser Performance in the Presence of Common Atmospheric Obscurants. Journal of Directed Energy*, 363-375.

Fiorino, S. T., Bartell, R. J., Perram, G. P., Manning, Z. P., Long, S. N., Houle, M. J., Krizo, M. J., Bunch, D. W., & Gravley, L. E. (2005). *Critical Assessment of Relative Humidity and Aerosol Effects on Lower Atmospheric High Energy Laser Engagement*, 3rd Annual Directed Energy Professional Society Modeling and Simulation Conference, Tampa, FL, March 2005.

Gebhardt, F. G. (1990). *Twenty Five Years of Thermal Blooming: An Overview.* SPIE Volume 1221 Propagation of High-Energy Laser Beams through the Earth's Atmosphere.

Gravley, L., Fiorino, S., Bartell, R., Perram, G., M.J. Krizo., & Le, K. (2007). Comparison of Climatological Optical Turbulence Profiles to Standard, Statistical, and Numerical Models Using HELEEOS. *Journal of Directed Energy*, 347-362.

Hecht, J. (2008, February 01). *LASER WEAPONS: Advanced tactical laser is ready for flight test (ATL vs. ABL)*. Retrieved August 25, 2008, from Laser Focus World: http://www.laserfocusworld.com/display_article/318547/12/none/none/News/LASER-WEAPONS:-Advanced-tactical-laser-is-ready-for-flight-test

Hess, M., Koepke, P., & Schult, I. (1998). Optical Properties of Aerosols and Clouds: The Software Package OPAC. *Bulletin of the American Meteorological Society* , 831-844.

Koepke, P., Hess, M., Schult, I., & Shettle, E. P. (1997). Global Aerosol Data Set. MPI Meteorologie Hamburg Report No. 243, 44 pp.

Missile Defense Agency (2008, June 01). *Missile Defense Agency*. Retrieved August 01, 2008, from The Airborne Laser Fact Sheet: http://www.mda.mil/mdalink/pdf/laser.pdf

Narcisse, D. L. (2008). *Optimizing Directed Energy Weapons Effectiveness with Specialized Weather Support.*

Petty, G. (2006). *A First Course In Atmospheric Radiation 2nd Edition.* Madison: Sundog Publishing.

Pries, T. (1990). High Energy Laser Meteorology (HELMET). *SPIE Vol. 1221* , 254-292.

Rutherford, M. (2008, August 18). *Military Tech*. Retrieved August 20, 2008, from Invisible Airborne Laser also'Deniable': http://news.cnet.com/8301-13639_3-10018808-42.html

Wallace, J. P., & Hobbs, P. V. (2006). *Atmospheric Science: An Introductory Survey.* San Diego: Academic Press.

Wirsig, G. W., & Fischer, D. (2008, May 30). *Federation of American Scientists*. Retrieved August 15, 2008, from Airborne Laser: http://www.fas.org/spp/starwars/program/abl.htm

REPORT DOCUMENTATION PAGE

Form Approved
OMB No. 074-0188

The public reporting burden for this collection of information is estimated to average 1 hour per response, including the time for reviewing instructions, searching existing data sources, gathering and maintaining the data needed, and completing and reviewing the collection of information. Send comments regarding this burden estimate or any other aspect of the collection of information, including suggestions for reducing this burden to Department of Defense, Washington Headquarters Services, Directorate for Information Operations and Reports (0704-0188), 1215 Jefferson Davis Highway, Suite 1204, Arlington, VA 22202-4302. Respondents should be aware that notwithstanding any other provision of law, no person shall be subject to an penalty for failing to comply with a collection of information if it does not display a currently valid OMB control number.
PLEASE DO NOT RETURN YOUR FORM TO THE ABOVE ADDRESS.

1. REPORT DATE *(DD-MM-YYYY)*	**2. REPORT TYPE**	**3. DATES COVERED** *(From – To)*
27-03-2009	Master's Thesis	Jun 2007-Mar 2009

4. TITLE AND SUBTITLE
Assessment of Weather Sensitivites and Air Force Weather (AFW) Support to Tactical Lasers in the Lower Troposphere

5a. CONTRACT NUMBER

5b. GRANT NUMBER

5c. PROGRAM ELEMENT NUMBER

6. AUTHOR(S)
Francesco J. Echeverria, Capt, USAF

5d. PROJECT NUMBER

5e. TASK NUMBER

5f. WORK UNIT NUMBER

7. PERFORMING ORGANIZATION NAMES(S) AND ADDRESS(S)
Air Force Institute of Technology
Graduate School of Engineering and Management (AFIT/EN)
2950 Hobson Way
WPAFB OH 45433-7765

8. PERFORMING ORGANIZATION REPORT NUMBER
AFIT/GAP/ENP/09-M05

9. SPONSORING/MONITORING AGENCY NAME(S) AND ADDRESS(ES)
Intentionally Left Blank

10. SPONSOR/MONITOR'S ACRONYM(S)

11. SPONSOR/MONITOR'S REPORT NUMBER(S)

12. DISTRIBUTION/AVAILABILITY STATEMENT
APPROVED FOR PUBLIC RELEASE; DISTRIBUTION UNLIMITED

13. SUPPLEMENTARY NOTES

14. ABSTRACT

ATL scientists need to develop a full understanding of the interaction effects between a high-energy laser beam and the atmosphere through which it propagates. Achieving this understanding is important for many reasons. In particular, the high cost of DE weapons systems makes each propagation event expensive. Having an understanding of the atmosphere in which a high-energy laser propagates will increase efficiency and effectiveness of the ATL weapon system, which in turn will decrease cost of operation. A tool that allows for the ATL war-fighter to determine the atmospheric effects on laser propagation currently does not exist. This study creates a stepping-stone toward creating a High Energy Laser Tactical Decision Aid (HELTDA) in which the war-fighter will be able to determine the effectiveness of the ATL weapon system with accuracy in order to maximize efficiency in a specific environment.

Using the High Energy Laser End-to-End Simulation (HELEEOS) software, comparisons are made across various atmospheric factors. These factors consist of a variety of turbulence and wind profiles, aerosol effects, time of day, clouds and rain, and relative humidity, which are compared for summer and winter for a specific mid-latitude geographic location. In addition, the atmospheric factors run in HELEEOS are used to determine and characterize the relevant attenuating factors of extinction and thermal blooming, which are inferred by the different engagement scenarios tested.

The results illustrate the three attenuation factors of high energy laser propagation: optical turbulence, extinction, and thermal blooming. In this study, the most significant attenuation factor is thermal blooming. Extinction is a significant attenuator as well, however, not to the degree of thermal blooming. Optical turbulence proved to be a negligible attenuator for increasingly vertical engagements. This is especially true for ATL engagements, which are generally limited to approximately 10km in slant range. The seasonal and time of day weather effects are also at times significant.

15. SUBJECT TERMS

16. SECURITY CLASSIFICATION OF:			**17. LIMITATION OF ABSTRACT**	**18. NUMBER OF PAGES**	**19a. NAME OF RESPONSIBLE PERSON**
REPORT	**ABSTRACT**	**c. THIS PAGE**			**Steven T. Fiorino, Lt Col, USAF**
U	**U**	**U**	**UU**	82	**19b. TELEPHONE NUMBER** *(Include area code)* *937-255-3636 x 4506 steven.fiorino@afit.edu*